Electronic Research Archive

https://www.aimspress.com/journal/era

ERA, 33(11): 6922–6951.
DOI: 10.3934/era.2025305
Received: 14 September 2025
Revised: 31 October 2025
Accepted: 11 November 2025
Published: 17 November 2025

Research article

Fixed-time control of switched memristor-based BAM neural networks with time-varying delays

Ziqing Yuan[1,*] **and Zuowei Cai**[2]

[1] Department of Applied Mathematics, Huaihua University, Huaihua 418000, China

[2] College of Information Science and Engineering, Hunan Women's University, Changsha 410002, China

* **Correspondence:** Email: 312917335@163.com.

Abstract: This study investigates the prespecified-/finite-time stability for a class of memristor-based BAM neural networks (MBAMNNs) with discontinuity. By C-regular Lyapunov approach stability theories, some criteria are established to ensure that the switched MBAMNNs can achieve prespecified-/finite-time stabilization, which are independent of the initial states. Finally, some numerical examples demonstrate the effectiveness of the proposed criteria. This work provides a theoretical foundation for precise temporal control in complex neural networks.

Keywords: BAM neural networks; prespecified-time stability; finite-time stability; external input controller

1. Introduction

The pursuit of neuromorphic computing and advanced artificial intelligence has driven the development of sophisticated neural network models that aim to emulate the complexity and efficiency of biological brains. A pivotal milestone in this journey was the theoretical proposition of the memristor by Chua [1], which completed the fundamental quartet of passive circuit elements. The physical realization of memristors by Hewlett-Packard [2] ignited widespread research interest due to unique their unique property where resistance is governed by the historical charge flow [3]. This memory characteristic is intrinsically analogous to synaptic plasticity, making memristor-based neural networks (MNNs) a highly promising platform for emulating complex brain functions [4–11]. In parallel, architectural innovations in neural networks have evolved, among which the BAM network, introduced by Kosko [12], is notable for its two-layer, fully interconnected structure. This architecture provides robust associative memory capabilities, enabling effective pattern recall even from incomplete or noisy inputs, and has found applications in pattern recognition, automatic control, and artificial

intelligence [13]. The combination of memristive dynamics with the BAM architecture, has given rise to memristor-based BAM neural networks (MBAMNNs), which present a rich framework for exploring advanced cognitive processes.

The practical deployment of MBAMNNs, and neural networks in general, hinges critically on their dynamic behaviors, with stability and synchronization being paramount. Real-world implementations are invariably subject to time delays due to finite signal transmission and processing speeds, which can degrade performance or even induce instability. Consequently, significant research efforts have been dedicated to developing rigorous stability analysis methods. The evolution of stability notions has progressed from finite-time stability (FNTS) [14–21], which ensures convergence within a bounded time that depends on initial conditions, to fixed-time stability (FXTS) [22], where the settling time is bounded regardless of initial states but is still influenced by system parameters. More recently, prespecified-time stability (PSTS) [23, 24] has been developed, which allows the convergence time to be pre-assigned explicitly as a user-defined parameter, independent of both initial conditions and system parameters, offering unparalleled precision for applications with strict temporal requirements. Theoretical underpinnings for PSTS have been strengthened through developments such as modified Lyapunov techniques [25, 26] and their extension to discontinuous systems via C-regular Lyapunov functions [27, 28], enabling applications in multi-agent systems [29], variable structure control [30], and optimal stabilization [31].

Complementing stability analysis, the design of control strategies has also seen substantial evolution. Event-triggered control mechanisms have emerged as a prominent approach to enhance resource efficiency in networked systems by updating control signals only when specific error thresholds are violated [32]. This is particularly valuable in stochastic environments [32] and when facing security challenges such as denial-of-service (DoS) attacks, where adaptive mechanisms are required to maintain synchronization [33]. Furthermore, the analysis of complex systems has been bolstered by methodological innovations, such as modeling delayed neural networks as switched systems based on the delay derivative [19] and deriving tighter stability conditions using generalized reciprocally convex inequalities [34].

Despite these significant advances, the application of PSTS to switched MBAMNNs with time-varying delays remains a challenging and relatively unexplored territory. The inherent discontinuous switching dynamics of memristors, which are typically modeled with state-dependent connection weights [35, 36], pose a fundamental challenge to conventional continuous analysis frameworks. Many existing stability analyses for neural networks often rely on the assumption of bounded activation functions [37], which can be restrictive. Moreover, while PSTS has been explored in some neural network contexts [23, 28], a comprehensive framework tailored for the discontinuous, delayed, and switched nature of MBAMNNs is still lacking. These challenges limit the potential of MBAMNNs in applications requiring exact timing control, such as real-time signal processing and secure communications [38–40].

In response to these challenges, this paper introduces a prespecified-time stability framework for switched MBAMNNs with time-varying delays. The main contributions of this work are summarized as follows:

i) **Novel controller design:** We propose a new control scheme specifically designed for the dual-layer structure of MBAMNNs to achieve PSTS. A key feature of our approach is the decoupling of the settling time from both the initial conditions and the specific parameters of the system,

allowing for precise pre-specification of the convergence time.

ii) **Discontinuous dynamics handling:** We explicitly account for the discontinuous nature of memristive connection weights, which switch based on the system states. Our stability analysis is developed using a framework that can handle these discontinuities effectively, moving beyond the limitations of models that assume continuous or Lipschitz continuous connection weights.

iii) **Relaxed activation function constraints:** Our stability criteria require the activation functions to be only Lipschitz continuous, relaxing the common assumption of boundedness [37]. This expands the applicability of our results to a broader class of neural networks.

The remainder of this paper is organized as follows. Section 2 presents the model formulation of the switched MBAMNN and necessary mathematical preliminaries. The main results on prespecified-time stability are detailed in Sections 3 and 4, and are validated by numerical simulations to verify the theoretical validity. Finally, Section 5 concludes the paper and discusses potential future research directions.

2. Preliminaries and problem formulation

This paper investigates the following switched memristor-based bidirectional associative memory neural networks (MBAMNNs) model with time-varying discrete delays [41, 42]:

$$\begin{cases} \dot{x}_p(t) = -\sigma_p(x_p(t))x_p(t) + \sum_{q=1}^{m} a_{qp}(x_p(t))f_q(y_q(t)) + \sum_{q=1}^{m} b_{qp}(x_p(t))f_q(y_j(t-\tau(t))) + u_p(t), \\ \dot{y}_q(t) = -\rho_q(y_q(t))y_q(t) + \sum_{p=1}^{n} c_{pq}(y_q(t))g_p(x_p(t)) + \sum_{p=1}^{n} d_{pq}(y_q(t))g_p(x_p(t-\tau(t))) + v_q(t), \end{cases} \tag{2.1}$$

for $p = 1, 2, \ldots, n$ and $q = 1, 2, \ldots, m$. Here, $x_p(t)$ and $y_q(t)$ denote the voltages capacitor C_p and $\hat{C}_q$, respectively; $u_p(t)$ and $v_q(t)$ represent external inputs; $\sigma_p(\cdot) > 0$ and $\rho_q(\cdot) > 0$ represent the self-inhibition rates of the neurons; $f_q(\cdot)$ and $g_p(\cdot)$ are the activation functions and $\tau(t)$ is the time-varying discrete delay satisfying $0 \le \tau(t) \le \tau$.

The memristive connection weights $a_{qp}(x_p(t))$, $\sigma_p(x_p(t))$, $b_{qp}(x_p(t))$, $c_{pq}(y_q(t))$, $d_{pq}(y_q(t))$, and $\rho_q(y_q(t))$ are defined as follows:

$$\sigma_p(x_p(t)) = \frac{1}{C_p}\left[\sum_{q=1}^{m}(M_{qp} + M^*_{qp}) \times \text{sign}_{qp} + \frac{1}{R_p}\right],$$

$$\rho_q(y_q(t)) = \frac{1}{\hat{C}_q}\left[\sum_{p=1}^{n}(\hat{M}_{pq} + \hat{M}^*_{pq}) \times \text{sign}_{pq} + \frac{1}{\hat{R}_q}\right],$$

$$a_{qp}(x_p(t)) = \frac{M_{qp}}{C_p} \times \text{sign}_{qp}, b_{qp}(x_p(t)) = \frac{M^*_{qp}}{C_p} \times \text{sign}_{qp},$$

$$c_{pq}(y_q(t)) = \frac{\hat{M}_{pq}}{\hat{C}_q} \times \text{sign}_{pq}, d_{pq}(y_q(t)) = \frac{\hat{M}^*_{pq}}{\hat{C}_q} \times \text{sign}_{pq},$$

where the signal function is defined by

$$\text{sign}_{qp} = \begin{cases} 1, & q \neq p, \\ -1, & q = p. \end{cases}$$

In these definitions, M_{qp}, $\hat{M}_{pq}$, M^*_{qp}, and $\hat{M}^*_{pq}$ denote the memductances of memristors R_{qp}, $\hat{R}_{pq}$, R^*_{qp}, and $\hat{R}^*_{pq}$, respectively. Specifically, R_{qp} is the memristor connecting $f_q(y_q(t))$ to $x_p(t)$, $\hat{R}_{pq}$ is the memristor connecting $g_p(x_p(t))$ to $y_q(t)$, R^*_{qp} is the memristor connecting $f_q(y_q(t-\tau(t)))$ to $x_p(t)$, and $\hat{R}^*_{pq}$ is the memristor connecting $g_p(x_p(t-\tau(t)))$ to $y_q(t)$. The terms R_p and $\hat{R}_q$ represent parallel resistors.

Based on the characteristics of memristive dynamics, we set

$$\sigma_p(v) = \begin{cases} \sigma'_p, & |v| \leq T_p, \\ \sigma''_p, & |v| > T_p, \end{cases} \rho_q(v) = \begin{cases} \rho'_q, & |v| \leq \hat{T}_q, \\ \rho''_q, & |v| > \hat{T}_q, \end{cases}$$

$$a_{qp}(v) = \begin{cases} a'_{qp}, & |v| \leq T_p, \\ a''_{qp}, & |v| > T_p, \end{cases} b_{qp}(v) = \begin{cases} b'_{qp}, & |v| \leq T_p, \\ b''_{qp}, & |v| > T_p, \end{cases}$$

$$c_{pq}(v) = \begin{cases} c'_{pq}, & |v| \leq \hat{T}_q, \\ c''_{pq}, & |v| > \hat{T}_q, \end{cases} d_{pq}(v) = \begin{cases} d'_{pq}, & |v| \leq \hat{T}_q, \\ d''_{pq}, & |v| > \hat{T}_q, \end{cases}$$

for $p = 1, 2, ..., n$, $q = 1, 2, ..., m$, where $T_p, \hat{T}_q$, σ'_p, ρ'_q, σ''_p, a'_{qp}, a''_{qp}, b'_{qp}, b''_{qp}, ρ''_j, c'_{pq},c''_{pq}, d''_{pq} and d''_{pq} are fixed constants.

Throughout this work, we define the following quantities for all $p = 1, 2, \ldots, n$ and $q = 1, 2, \ldots, m$:

$$\underline{\sigma}_p = \min\{\sigma'_p, \sigma''_p\}, \quad \underline{\rho}_q = \min\{\rho'_q, \rho''_q\},$$

$$a^u_{qp} = \max\{|a'_{qp}|, |a''_{qp}|\}, \quad b^u_{qp} = \max\{|b'_{qp}|, |b''_{qp}|\},$$
$$c^u_{pq} = \max\{|c'_{pq}|, |c''_{pq}|\}, \quad d^u_{pq} = \max\{|d'_{pq}|, |d''_{pq}|\}.$$

Additionally, let

$$\mathbb{N}_1 = \{1, 2, \ldots, n\}, \quad \mathbb{N}_2 = \{1, 2, \ldots, m\}.$$

The set of real numbers is denoted by $\mathbb{R}$, while $\mathbb{R}_+$ represents the nonnegative real numbers. The collection of all nonempty subsets of $\mathbb{R}^n$ is written as $2^{\mathbb{R}^n}$. For any vector $x \in \mathbb{R}^n$, its norm is expressed as $\|x\|$. If ϑ is a function, then ϑ^{-1} refers to its inverse.

Consider the non-autonomous time-delay functional system (TDFS):

$$\frac{\mathrm{d}x}{\mathrm{d}t} = f(t, x(t), x(t - \tau(t))), \tag{2.2}$$

where $x(t) \in \mathbb{R}^n$ denotes the system state, and $\tau(t)$ is a time-varying delay satisfying $0 \leq \tau(t) \leq \tau < +\infty$. The function $f : \mathbb{R} \times \mathbb{R}^n \times \mathbb{R}^n \to \mathbb{R}^n$ is assumed to be measurable and essentially locally bounded. The initial condition is given by a continuous function φ defined on the interval $[t_0 - \tau, t_0]$, such that

$$x(\theta) = \varphi(\theta), \quad \theta \in [t_0 - \tau, t_0],$$

where $t_0 \geq 0$ represents the initial time.

Definition 2.1 ([43]). On the interval $[0, T)$, a function $x(t)$ is said to be a Filippov solution of the TDFS given in (2.2) if it is absolutely continuous and satisfies the differential inclusion

$$\dot{x}(t) \in F(t, x(t), x(t - \tau(t)))$$

for almost every $t \in [0, T)$, where the set-valued map F is defined by

$$F(\xi, y, z) = \bigcap_{\varepsilon_1, \varepsilon_2 > 0} \bigcap_{\substack{\mu(N)=0 \\ \mu(M)=0}} \overline{\text{co}}\left[f(\xi, B(y, \varepsilon_1) \setminus N, B(z, \varepsilon_2) \setminus M)\right].$$

In this definition, μ denotes the Lebesgue measure, $B(p, r)$ represents the ball of radius r centered at point p, and $\overline{\text{co}}$ indicates the closed convex hull. The sets $N, M \subset \mathbb{R}^n$ are exceptional sets of measure zero.

Definition 2.2 ([43]). $\forall t \in \mathbb{R}$, if $0 \in F(t, 0, 0)$, then the origin $x = 0$ is defined for TDFS (2.2) via Filippov solution.

Definition 2.3 ([25]). The zero solution of (2.2) is termed prespecified-time attractive provided that its trajectory converges exactly to the origin at the fixed time $\mathcal{T}_p > 0$, i.e., $\lim_{t \to \mathcal{T}_p} x(t) = 0$, and remains there identically zero for all $t \geq \mathcal{T}_p$. Notably, this convergence time $\mathcal{T}_p$ is independent of both the initial conditions and any system parameters.

Definition 2.4 ([25]). The zero solution of (2.2) is said to be prespecified-time stable (PSTS) provided that it is both stable and prespecified-time attractive.

Since system (2.2) contains time-varying delays $\tau(t)$, its solution depends not only on the current state $x(t)$, but also on historical states $x(t - \tau(t))$. Therefore, initial conditions must be extended to the functional form.

Definition 2.5 ([44, 45]). The space $C = C([t_0 - \tau, t_0], \mathbb{R}^n)$ denotes a Banach space equipped with the norm

$$\|\varphi\|_C = \sup_{t_0 - \tau \leq s \leq t_0} \|\varphi(s)\|,$$

and consists of all continuous functions $\varphi : [t_0 - \tau, t_0] \to \mathbb{R}^n$, where each φ serves as an initial history function in this Banach space. The origin of the TDFS (2.2) is said to be:

•Stable if for every $\varepsilon > 0$ and every $t_0 \geq 0$, there exists $\delta = \delta(\varepsilon, t_0) > 0$ such that $\|x(t_0, \varphi)(t)\| < \varepsilon$ for all $\varphi \in B(0, \delta) = \{\varphi \in C : \|\varphi\|_C < \delta\}$ and all $t \geq t_0$. If δ is independent of t_0 , the system is uniformly stable at the origin.

• Attractive if for every $t_0 \geq 0$, there exists $\delta = \delta(t_0) > 0$ such that $\lim_{t \to +\infty} \|x(t_0, \varphi)(t)\| = 0$ for all $\varphi \in B(0, \delta)$. Equivalently, for every $\varepsilon > 0$ and $t_0 \in \mathbb{R}_+$, there exist $\delta = \delta(t_0) > 0$ and $T = T(\varepsilon, t_0, \varphi) > 0$ such that $\|x(t_0, \varphi)(t)\| < \varepsilon$ for all $\varphi \in B(0, \delta)$ and all $t \geq t_0 + T$. If T is independent of t_0 and φ, the system is uniformly attractive at the origin. If δ can be chosen arbitrarily large, the system is termed globally (uniformly) attractive.

Definition 2.6 ([43]). The Filippov solutions of the TDFS (2.2) are uniformly bounded if, for every $\delta > 0$, there exists a constant $M = M(\delta) > 0$ such that

$$\|x(t_0, \varphi)(t)\| \leq M$$

for all initial functions φ satisfying $\|\varphi\|_C < \delta$ and for all $t \geq t_0$.

Definition 2.7 ([46]). The origin is said to be finite-time attractive (FNTA) for the TDFS (2.2) if, for any initial condition, there exists a finite settling time $0 \le T(t_0, \varphi) < +\infty$ such that

$$\lim_{t \to T(t_0,\varphi)} x(t_0, \varphi)(t) = 0$$

and the state remains identically zero for all $t \ge T(t_0, \varphi)$.

Definition 2.8 ([46]). The origin is said to be fixed-time attractive (FXTA) for the time-delay functional system (TDFS) (2.2) if it is finite-time attractive (FNTA) and the settling time $T(t_0, \varphi)$ is bounded uniformly over all initial functions $\varphi \in C([t_0 - \tau, t_0], \mathbb{R}^n)$. That is, there exists a constant $T_{\max} > 0$ such that

$$T(t_0, \varphi) \le t_0 + T_{\max}$$

holds for every admissible φ.

Definition 2.9 ([47]). Let $V : \mathbb{R} \times \mathbb{R}^n \to \mathbb{R}$ be a locally Lipschitz continuous function, and let $\Omega_V \subset \mathbb{R}^n$ denote the set of points where V fails to be differentiable. The generalized gradient of V at a point $x \in \mathbb{R}^n$ is defined as

$$\partial V(x) = \overline{\text{co}} \left\{ \lim_{k \to \infty} \nabla V(x_k) : x_k \to x,\ x_k \notin O \cup \Omega_V \right\},$$

where $O \subset \mathbb{R}^n$ is an arbitrary set of Lebesgue measure zero.

Lemma 2.1. *([48, 49])* Suppose $V : \mathbb{R}^n \to \mathbb{R}$ is a C-regular function and $\mathbf{x}(t) : [t_0, +\infty) \to \mathbb{R}^n$ is absolutely continuous. Then, $\mathbf{x}(\mathbf{t})$ and the composition $V(\mathbf{x}(t)) : [t_0, +\infty) \to \mathbb{R}$ are differentiable almost everywhere on $[t_0, +\infty)$, and the derivative satisfies

$$\frac{\mathrm{d}V(\mathbf{x}(t))}{\mathrm{d}t} = \left\langle \xi(t), \frac{\mathrm{d}\mathbf{x}(t)}{\mathrm{d}t} \right\rangle, \forall \xi(t) \in \partial V(\mathbf{x}(t)). \tag{2.3}$$

for any $\xi(t) \in \partial V(\mathbf{x}(t))$.

Definition 2.10 (C-regularity [48, 50]). A function $V : \mathbb{R}^n \to \mathbb{R}$ is said to be C-regular if it satisfies the following properties:

(a) V is regular;
(b) $V(x) > 0$ for all $x \neq 0$, and $V(0) = 0$;
(c) $V(x) \to +\infty$ as $\|x\| \to +\infty$.

Let $\partial_t V(t, x)$ and $\partial_x V(t, x)$ represent the Clarke generalized gradients of $V(t, x)$ with respect to t and x, respectively. Analogous to the chain rule, the following lemma holds for the TDFS (2.2).

Lemma 2.2 ([47]). Let $x(t)$ be a Filippov solution of the time-delay functional system TDFS (2.2) on $t \in \mathbb{U}$, and suppose $V : \mathbb{R} \times \mathbb{R}^n \to \mathbb{R}$ is a C-regular function. Then, $x(t)$ and $V(t, x(t))$ are differentiable for almost every $t \in \mathbb{U}$, and

$$\frac{\mathrm{d}}{\mathrm{d}t} V(t, x(t))\Big|_{(2.2)} = \eta + \zeta^{\mathrm{T}} \gamma(t), \quad \text{for all } \eta \in \partial_t V(t, x),\ \zeta \in \partial_x V(t, x),$$

where $\gamma(t) \in F(t, x(t), x(t - \tau(t)))$ is a measurable function satisfying $\dot{x}(t) = \gamma(t)$ for almost every $t \in \mathbb{U}$.

Lemma 2.3 ([46]). Given nonnegative real numbers $\zeta_1, \zeta_2, \ldots, \zeta_n$ and exponents satisfying $0 < p < q$, then the following inequality holds:

$$n^{\frac{1}{p}-\frac{1}{q}}\left(\sum_{p=1}^{n}\zeta_p^q\right)^{1/q} \geq \left(\sum_{p=1}^{n}\zeta_p^p\right)^{1/p} \geq \left(\sum_{p=1}^{n}\zeta_p^q\right)^{1/q}.$$

Lemma 2.4 ([51]). Given nonnegative real numbers $x_1, x_2, \ldots, x_n \geq 0$, and exponents $0 < p \leq 1 < q$, then the following inequality holds:

$$\sum_{p=1}^{n} x_p^p \geq \left(\sum_{p=1}^{n} x_p\right)^p.$$

Proposition 2.1. *([52]) Let $\mathcal{T}_p > 0$ be a prespecified time. If a C-regular Lyapunov function $V : \mathbb{R}^n \to \mathbb{R}$ satisfies*

$$\frac{\mathrm{d}V}{\mathrm{d}t} \leq -\frac{\pi}{\mathcal{T}_p}(1+V)V^{1/2}$$

for almost every $t \geq 0$, then the origin of system (2.2) is PSTS.

3. The main results

Before presenting our main conclusions, we need the following assumptions:

(H1) The f_q and g_p satisfy $f_q(0) = 0$ and $g_p(0) = 0$, and for any $s, s^* \in \mathbb{R}$, $p, q \in \mathbb{N}$, there exist $L_q > 0$ and $\hat{L}_p > 0$ such that

$$|f_q(s) - f_q(s^*)| \leq L_q|s - s^*| \text{ and } |g_p(s) - g_p(s^*)| \leq \hat{L}_p|s - s^*|.$$

We say that $x(t)$ and $y(t)$ are the solution of (2.1) with initial values $x(0) = x_0$ and $y(0) = y_0$, if

$$\begin{cases} \dot{x}_p \in -\overline{\mathrm{co}}[\sigma_p(x_p(t))]x_p(t) + \sum_{q=1}^{m}\overline{\mathrm{co}}[a_{qp}(x_p(t))]f_q(y_q(t)) + \sum_{q=1}^{m}\overline{\mathrm{co}}[b_{qp}(x_p(t))]f_q(y_q(t-\tau(t))) \\ \qquad + u_p(t) \triangleq F_p(t,x), \\ \dot{y}_q \in -\overline{\mathrm{co}}[\rho_q(y_q(t))]y_q(t) + \sum_{p=1}^{n}\overline{\mathrm{co}}[c_{pq}(y_q(t))]g_p(x_p(t)) + \sum_{p=1}^{n}\overline{\mathrm{co}}[d_{pq}(y_q(t))]g_p(x_p(t-\tau(t))) \\ \qquad + v_q(t) \triangleq \hat{F}_q(t,y), \end{cases} \tag{3.1}$$

$p = 1, 2, ..., n$, $q = 1, 2, ..., m$, where

$$\overline{\mathrm{co}}[\sigma_p(x_p(t))] = \begin{cases} \hat{\sigma}_p, & |x_p(t)| < \varrho_p, \\ [\underline{\sigma}_p, \overline{\sigma}_p], & |x_p(t)| = \varrho_p, \\ \tilde{\sigma}_p, & |x_p(t)| > \varrho_p, \end{cases} \quad \overline{\mathrm{co}}[a_{qp}(x_p(t))] = \begin{cases} \hat{a}_{qp}, & |x_p(t)| < \varrho_p, \\ [\underline{a}_{qp}, \overline{a}_{qp}], & |x_p(t)| = \varrho_p, \\ \tilde{a}_{qp}, & |x_p(t)| > \varrho_p, \end{cases}$$

$$\overline{\mathrm{co}}[b_{qp}(x_p(t))] = \begin{cases} \hat{b}_{qp}, & |x_p(t)| < \varrho_p, \\ [\underline{b}_{qp}, \overline{b}_{qp}], & |x_p(t)| = \varrho_p, \\ \tilde{b}_{qp}, & |x_p(t)| > \varrho_p, \end{cases} \quad \overline{\mathrm{co}}[\rho_q(y_q(t))] = \begin{cases} \hat{\rho}_q, & |y_q(t)| < \hat{\varrho}_q, \\ [\underline{\rho}_q, \overline{\rho}_p], & |y_q(t)| = \hat{\varrho}_q, \\ \tilde{\rho}_p, & |y_q(t)| > \hat{\varrho}_q, \end{cases}$$

$$\overline{\mathrm{co}}[c_{pq}(y_q(t))] = \begin{cases} \hat{c}_{pq}, & |y_q(t)| < \hat{\varrho}_q, \\ [\underline{c}_{pq}, \overline{c}_{pq}], & |y_q(t)| = \hat{\varrho}_q, \\ \tilde{c}_{pq}, & |y_q(t)| > \hat{\varrho}_q, \end{cases} \quad \overline{\mathrm{co}}[d_{pq}(y_q(t))] = \begin{cases} \hat{d}_{pq}, & |y_q(t)| < \hat{\varrho}_q, \\ [\underline{d}_{pq}, \overline{d}_{pq}], & |y_q(t)| = \hat{\varrho}_q, \\ \tilde{d}_{pq}, & |y_q(t)| > \hat{\varrho}_q, \end{cases}$$

where $\underline{\sigma}_p = \min\{\hat{\sigma}_p, \tilde{\sigma}_p\}$, $\overline{\sigma}_p = \max\{\hat{\sigma}_p, \tilde{\sigma}_p\}$, $\underline{a}_{qp} = \min\{\hat{a}_{qp}, \tilde{a}_{qp}\}$, $\overline{a}_{qp} = \max\{\hat{a}_{qp}, \tilde{a}_{qp}\}$, $\underline{b}_{qp} = \min\{\hat{b}_{qp}, \tilde{b}_{qp}\}$, $\overline{b}_{qp} = \max\{\hat{b}_{qp}, \tilde{b}_{qp}\}$, $\underline{\rho}_j = \min\{\hat{\rho}_j, \tilde{\rho}_j\}$, $\overline{\rho}_{pq} = \max\{\hat{\rho}_j, \tilde{\rho}_j\}$, $\underline{c}_{pq} = \min\{\hat{c}_{pq}, \tilde{c}_{pq}\}$, $\overline{c}_{pq} = \max\{\hat{c}_{pq}, \tilde{c}_{pq}\}$, $\underline{d}_{pq} = \min\{\hat{d}_{pq}, \tilde{d}_{pq}\}$, and $\overline{d}_{pq} = \max\{\hat{d}_{pq}, \tilde{d}_{pq}\}$ for $p \in \mathbb{N}_1$ and $q \in \mathbb{N}_2$. It can be readily verified that the set-valued mapping

$$(t, x, y) \mapsto \left(F_1(t, x), \ldots, F_n(t, x), \widehat{F}_1(t, y), \ldots, \widehat{F}_m(t, y)\right)$$

has nonempty, compact, and convex values and is upper semicontinuous. As a result, the mapping is measurable (see [53]). By the measurable selection theorem (cf. Theorem 1 in [53]), there exist measurable selections $\xi_p(t) \in \overline{\text{co}}[\sigma_p(x_p(t))]$, $\alpha_{qp}(t) \in \overline{\text{co}}[a_{qp}(x_p(t))]$, $\beta_{qp}(t) \in \overline{\text{co}}[b_{qp}(x_p(t))]$, $\iota_q(t) \in \overline{\text{co}}[\rho_q(y_q(t))]$, $\mu_{pq}(t) \in \overline{\text{co}}[c_{pq}(y_q(t))]$ and $\nu_{qp}(t) \in \overline{\text{co}}[d_{pq}(y_q(t))]$ such that for a.e. $t \geq 0$,

$$\begin{cases} \dot{x}_p = -\xi_p(t)x_p(t) + \sum_{q=1}^m \alpha_{qp}(t)f_q(y_q(t)) + \sum_{q=1}^m \beta_{qp}(t)f_q(y_q(t-\tau(t))) + u_p(t) \\ \dot{y}_q = -\iota_q(t)y_q(t) + \sum_{p=1}^n \mu_{pq}(t)g_p(x_p(t)) + \sum_{p=1}^n \nu_{qp}(t)g_p(x_p(t-\tau(t))) + v_q(t). \end{cases} \tag{3.2}$$

3.1. The PST stabilization Theorem

Design the prespecified-time external control protocols as

$$\begin{aligned} u_p(t) &= -\lambda_p x_p(t) - \Lambda_p|x_p(t-\tau(t))|sign(x_p(t)) - \frac{\pi}{\mathcal{T}_p}(1 + \|x(t)\| + \|y(t)\|)|x_(t)|^{\frac{1}{2}} sign(x_p(t)) \\ v_q(t) &= -\mu_q y_q(t) - \beth_q|y_q(t-\tau(t))|sign(y_q(t)) - \frac{\pi}{\mathcal{T}_p}(1 + \|x(t)\| + \|y(t)\|)|y(t)|^{\frac{1}{2}} sign(y_q(t)), \end{aligned} \tag{3.3}$$

where $\|x(t)\| \triangleq \sum_{p=1}^n |x_p(t)|$, $\|y(t)\| \triangleq \sum_{q=1}^m |y_q(t)|$, $\mathcal{T}_p$ is a prespecified time, and the control gains $\lambda_p \geq 0$, $\mu_q \geq 0$, $\Lambda_p \geq 0$, and $\beth_q \geq 0$.

Theorem 3.1. *If assumption (H1) holds and the following conditions are satisfied*

(H2) for all $p \in \mathbb{N}_1$, $q \in \mathbb{N}_2$, $-\underline{\sigma}_p + \sum_{q=1}^m c_{pq}^u \hat{L}_p - \lambda_p \leq 0$, *and* $-\underline{\rho}_q + \sum_{p=1}^n a_{qp}^u L_q - \mu_q \leq 0$;
(H3) for all $p \in \mathbb{N}_1$, $q \in \mathbb{N}_2$, $\sum_{p=1}^n b_{qp}^u - \beth_q \leq 0$, *and* $\sum_{q=1}^m d_{pq}^u - \Lambda_p \leq 0$,

the zero of BAM (2.1) achieves prespecified-time stability within the predefined time T_p *under protocol (3.3).*

Proof. Choose the following Lyapunov function:

$$V(t) = V_1(t) + V_2(t), \tag{3.4}$$

where

$$V_1(t) = \sum_{p=1}^n |x_p(t)| = \|x(t)\| \text{ and } V_2(t) = \sum_{q=1}^m |y_q(t)| = \|y(t)\|. \tag{3.5}$$

Obviously, V has C-regularity. Employing Lemma 2.1, we can compute

$$\begin{aligned}
\frac{dV_1}{dt} &= \sum_{p=1}^{n} \frac{dx_p}{dt} sign(x_p(t)) \\
&= \sum_{p=1}^{n} [-\sigma_p(x_p(t))x_p(t) + \sum_{q=1}^{m} a_{qp}(x_p(t))f_q(y_q(t)) + \sum_{q=1}^{m} b_{qp}(x_p(t))f_q(y_q(t-\tau(t))) + u_p(t)]sign(x_p(t)) \\
&\leq -\sum_{p=1}^{n} \underline{\sigma}_p|x_p(t)| + \sum_{p=1}^{n}\sum_{q=1}^{m} a^u_{qp}|f_q(y_q(t))| + \sum_{p=1}^{n}\sum_{q=1}^{m} b^u_{qp}|f_q(y_q(t-\tau(t)))| + \sum_{p=1}^{n} u_p(t)sign(x_p(t)) \\
&\leq -\sum_{p=1}^{n} \underline{\sigma}_p|x_p(t)| + \sum_{p=1}^{n}\sum_{q=1}^{m} a^u_{qp}L_q|y_q(t)| + \sum_{p=1}^{n}\sum_{q=1}^{m} b^u_{qp}L_q|y_q(t-\tau(t))| + \sum_{p=1}^{n} u_p(t)sign(x_p(t))
\end{aligned} \tag{3.6}$$

for a.e. $0 \leq t$.

Similarly, we obtain

$$\frac{dV_2}{dt} \leq -\sum_{q=1}^{m} \underline{\rho}_q|y_q(t)| + \sum_{q=1}^{m}\sum_{p=1}^{n} c^u_{qp}\hat{L}_p|x_p(t)| + \sum_{q=1}^{m}\sum_{p=1}^{n} d^u_{qp}L_q|x_p(t-\tau(t))| + \sum_{q=1}^{m} v_q(t)sign(y_q(t)) \tag{3.7}$$

for a.e. $0 \leq t$. Then, from (H2), (H3), and (3.3), it follows that

$$\begin{aligned}
\frac{dV}{dt} \leq & \sum_{p=1}^{n} |x_p(t)|[\underline{\sigma}_p + \sum_{q=1}^{m} c^u_{pq}\hat{L}_p - \lambda_p] + \sum_{q=1}^{m} |y_q(t)|[\underline{\rho}_q + \sum_{p=1}^{n} a^u_{qp}L_q - \mu_q] \\
& + \sum_{q=1}^{m} \Big(\sum_{p=1}^{n} b^u_{qp} - \beth_q \Big)|y_q(t-\tau(t))| + \sum_{p=1}^{n} \Big(\sum_{q=1}^{m} d^u_{pq} - \Lambda_p \Big)|x_p(t-\tau(t))| \\
& - \sum_{p=1}^{n} \frac{\pi}{\mathcal{T}_p}(1 + \|x\| + \|y\|)|x_p(t)|^{\frac{1}{2}} - \sum_{q=1}^{m} \frac{\pi}{\mathcal{T}_p}(1 + \|x\| + \|y\|)|y_q(t)|^{\frac{1}{2}}.
\end{aligned} \tag{3.8}$$

Consequently,

$$\begin{aligned}
\frac{dV}{dt} &\leq -\sum_{p=1}^{n} \frac{\pi}{\mathcal{T}_p}(1 + \|x\| + \|y\|)|x_p(t)|^{\frac{1}{2}} - \sum_{q=1}^{m} \frac{\pi}{\mathcal{T}_p}(1 + \|x\| + \|y\|)|y_q(t)|^{\frac{1}{2}} \\
&\leq -\frac{\pi}{\mathcal{T}_p}(1 + \|x\| + \|y\|)(\|x(t)\| + \|y(t)\|)^{\frac{1}{2}} \\
&= -\frac{\pi}{\mathcal{T}_p}(+V(t))V(t)^{\frac{1}{2}}.
\end{aligned} \tag{3.9}$$

From Proposition 2.1, we known that the zero of BAM (2.1) is PST stabilized within a prespecified-time $\mathcal{T}_p$ under protocol (3.3).

In the following, we present the second result.

3.2. The PST stabilization theorem

Design the prespecified-time external control protocols as

$$\begin{aligned} u_p(t) &= -\lambda_p x_p(t) - \Lambda_p |x_p(t-\tau(t))| sign(x_p(t)) - \frac{T_2^{\max}}{\mathcal{T}_p}(e^{(\|x(t)\|+\|y(t)\|)^{\frac{1}{2}}} + 1)|x_p(t)|^{\frac{1}{2}} sign(x_p(t)) \\ v_q(t) &= -\mu_q y_q(t) - \beth_q |y_q(t-\tau(t))| sign(y_q(t)) - \frac{T_2^{\max}}{\mathcal{T}_p}(e^{(\|x(t)\|+\|y(t)\|)^{\frac{1}{2}}} + 1)|y_q(t)|^{\frac{1}{2}} sign(y_q(t)), \end{aligned} \tag{3.10}$$

where $\|x(t)\| = \sum_{p=1}^{n} |x_p(t)|$ and $\|y(t)\| = \sum_{q=1}^{m} |y_q(t)|$. Here, $\mathcal{T}_p$ represents the pre-specified time, and the control gains $\lambda_p \geq 0$, $\mu_q \geq 0$, $\Lambda_p \geq 0$, and $\beth_q \geq 0$ are parameters which will be determined later.

Theorem 3.2. *If assumptions (H1)–(H3) hold, then the zero of BAM (2.1) achieves prespecified-time stability within the predefined time $\mathcal{T}_p$ with the control protocols (3.10).*

Proof. Choose the following Lyapunov function:

$$V(t) = V_1(t) + V_2(t), \tag{3.11}$$

where

$$V_1(t) = \sum_{p=1}^{n} |x_p(t)| = \|x(t)\|, \text{ and } V_2(t) = \sum_{q=1}^{m} |y_q(t)| = \|y(t)\|. \tag{3.12}$$

Obviously, V has C-regularity. Using Lemma 2.1 and (H1), we can derive

$$\begin{aligned} \frac{dV_1}{dt} &= \sum_{p=1}^{n} \frac{dx_p}{dt} sign(x_p(t)) \\ &= \sum_{p=1}^{n} [-\sigma_p(x_p(t))x_p(t) + \sum_{q=1}^{m} a_{qp}(x_p(t))f_q(y_q(t)) + \sum_{q=1}^{m} b_{qp}(x_p(t))f_q(y_q(t-\tau(t))) + u_p(t)] sign(x_p(t)) \\ &\leq -\sum_{p=1}^{n} \underline{\sigma}_p |x_p(t)| + \sum_{p=1}^{n}\sum_{q=1}^{m} a_{qp}^u |f_q(y_q(t))| + \sum_{p=1}^{n}\sum_{q=1}^{m} b_{qp}^u |f_q(y_q(t-\tau(t)))| + \sum_{p=1}^{n} u_p(t) sign(x_p(t)) \\ &\leq -\sum_{p=1}^{n} \underline{\sigma}_p |x_p(t)| + \sum_{p=1}^{n}\sum_{q=1}^{m} a_{qp}^u L_q |y_q(t)| + \sum_{p=1}^{n}\sum_{q=1}^{m} b_{qp}^u L_q |y_q(t-\tau(t))| + \sum_{p=1}^{n} u_p(t) sign(x_p(t)) \end{aligned} \tag{3.13}$$

for a.e. $0 \leq t$.

Similarly, we can obtain

$$\frac{dV_2}{dt} \leq -\sum_{q=1}^{m} \underline{\rho}_q |y_q(t)| + \sum_{q=1}^{m}\sum_{p=1}^{n} c_{qp}^u \hat{L}_p |x_p(t)| + \sum_{q=1}^{m}\sum_{p=1}^{n} d_{qp}^u L_q |x_p(t-\tau(t))| + \sum_{q=1}^{m} v_q(t) sign(y_q(t)) \tag{3.14}$$

for a.e. $t \geq 0$. Then, from (3.13) and (3.14), it follows that

$$\begin{aligned}\frac{dV}{dt} \leq & \sum_{p=1}^{n}|x_p(t)|\Big[\underline{\sigma}_p + \sum_{q=1}^{m} c_{pq}^{u}\hat{L}_p - \lambda_p\Big] + \sum_{q=1}^{m}|y_q(t)|\Big[\underline{\rho}_q + \sum_{p=1}^{n} a_{qp}^{u}L_q - \mu_q\Big] \\ & + \sum_{q=1}^{m}\Big(\sum_{p=1}^{n} b_{qp}^{u} - \mu_q\Big)|y_q(t-\tau(t))| + \sum_{p=1}^{n}\Big(\sum_{q=1}^{m} d_{pq}^{u} - \Lambda_p\Big)|x_p(t-\tau(t))| \\ & - \sum_{p=1}^{n}\frac{T_2^{\max}}{\mathcal{T}_p}\Big(e^{(\|x(t)\|+\|y(t)\|)^{\frac{1}{2}}}+1\Big)|x_p(t)|^{\frac{1}{2}} - \sum_{q=1}^{m}\frac{T_2^{\max}}{\mathcal{T}_p}\Big(e^{(\|x(t)\|+\|y(t)\|)^{\frac{1}{2}}}+1\Big)|y_q(t)|^{\frac{1}{2}}.\end{aligned} \tag{3.15}$$

Consequently,

$$\begin{aligned}\frac{dV}{dt} &\leq -\sum_{p=1}^{n}\frac{T_2^{\max}}{\mathcal{T}_p}\Big(e^{(\|x(t)\|+\|y(t)\|)^{\frac{1}{2}}}+1\Big)|x_p(t)|^{\frac{1}{2}} - \sum_{q=1}^{m}\frac{T_2^{\max}}{\mathcal{T}_p}\Big(e^{(\|x(t)\|+\|y(t)\|)^{\frac{1}{2}}}+1\Big)|y_q(t)|^{\frac{1}{2}} \\ &\leq -\frac{T_2^{\max}}{\mathcal{T}_p}\Big(e^{(\|x(t)\|+\|y(t)\|)^{\frac{1}{2}}}+1\Big)(\|x(t)\|+\|y(t)\|)^{\frac{1}{2}} \\ &= -\frac{T_2^{\max}}{\mathcal{T}_p}\Big(e^{V(t)^{\frac{1}{2}}}+1\Big)V(t)^{\frac{1}{2}}.\end{aligned} \tag{3.16}$$

From Theorem 2 in [52], we known that the zero of BAM (2.1) is PST stabilized within a prespecified-time $\mathcal{T}_p$ under the control protocols (3.10).

The two aforementioned results primarily delve into the PST stability of system (2.1). Building upon this foundation, we now present two conclusions regarding the finite-time convergence of system (2.1).

3.3. The FNTS and FXTS theorems

Consider the case where $u_p(t) = 0$, $v_q(t) = 0$, $x = (0,\ldots,0)^T$, and $y = (0,\ldots,0)^T$. Under these conditions, the trivial state solution of the BAM system (2.1) is achieved. To ensure that this trivial state solution exhibits FNTS/FXTS, we propose two distinct classes of switching control strategies, $u(t) = (u_1(t),\ldots,u_n(t))^T$ and $v(t) = (v_1(t),\ldots,v_m(t))^T$, as follows:

Case (i): For $p \in \mathbb{N}_1$ and $q \in \mathbb{N}_2$,

$$u_p(t) = \tilde{a}_p x_p(t) - \tilde{b}_p|x_p(t-\tau(t))|sign(x_p(t)) + \mathcal{D}(t)x_p(t) - \mathcal{P}(t)|x_p(t)|^{\beta}sign(x_p(t)) \tag{3.17}$$

and

$$v_q(t) = \hat{a}_q y_q(t) - \hat{b}_q|y_q(t-\tau(t))|sign(y_q(t)) + \mathcal{D}(t)y_q(t) - \mathcal{P}(t)|y_q(t)|^{\beta}sign(y_q(t)), \tag{3.18}$$

where $0 < \beta < 1$, the coefficients $\tilde{a}_p$, $\hat{a}_q$, $\tilde{b}_p$, and $\hat{b}_q$ represent constant control gains, and $\mathcal{P} > 0$ and $\mathcal{D}$ are time-varying control.

Case (ii): For $p \in \mathbb{N}_1$ and $q \in \mathbb{N}_2$,

$$\begin{aligned}u_p(t) = & \tilde{a}_p x_p(t) - \tilde{b}_p|x_p(t-\tau(t))|sign(x_p(t)) + \mathcal{D}(t)x_p(t) - \mathcal{P}(t)|x_p(t)|^{\beta}sign(x_p(t)) \\ & - \mathcal{P}(t)|x_p(t)|^{\gamma}sign(x_p(t))\end{aligned} \tag{3.19}$$

and

$$v_q(t) = \hat{a}_q y_q(t) - \hat{b}_q|y_q(t-\tau(t))|sign(y_q(t)) + \mathcal{D}(t)y_q(t) - \mathcal{P}(t)|y_q(t)|^{\beta}sign(y_q(t)) - \mathcal{P}(t)|y_q(t)|^{\gamma}sign(y_q(t)) \tag{3.20}$$

where $0 < \beta, \gamma < 1$, the parameters $\tilde{a}_p$, $\hat{a}_q$, $\tilde{b}_p$, and $\hat{b}_q$ represent constant control gains, $\mathcal{P} > 0$ and $\mathcal{D}$ denote time-varying control.

Give the following hypothesis:

(S) $\int_0^{+\infty} \mathcal{D}^M(s)ds < +\infty$, where $\mathcal{D}^M(s) = \max\{\mathcal{D}(s), 0\}$ and there exists a $\lambda > 0$ such that

$$\int_0^t \mathcal{P}(s)ds \geq \lambda(t - t_0) \ \ \forall t \geq t_0.$$

Theorem 3.3. *Assume conditions (H1) and (S) are satisfied. For $p \in \mathbb{N}_1$ and $q \in \mathbb{N}_2$, the following inequalities are satisfied:*

(H4) $-\underline{\sigma}_p + \sum_{q=1}^m c_{pq}^u \hat{L}_p - \tilde{a}_p \leq 0$ *and* $-\underline{\rho}_q + \sum_{p=1}^n a_{qp}^u L_q - \hat{a}_q \leq 0$*;*

(H5) $\sum_{p=1}^n b_{qp}^u L_q - \hat{b}_q \leq 0$ *and* $\sum_{q=1}^m d_{pq}^u \hat{L}_p - \Lambda_p \leq 0$.

Then, the trivial state solution of BAM (2.1) has uniform FNTS under control protocols (3.17) and (3.18). Furtheormore, the settling time satisfies

$$T(t_0, x_{t_0}, y_{t_0}) = t_0 + \frac{(\|x(t_0)\| + \|y(t_0)\|)^{1-\beta}}{(1-\beta)H^*\lambda},$$

where $H^* = e^{-(1-\beta)/2\int_0^{+\infty} \mathcal{D}^M(s)ds}$.

Proof. Choose following Lyapunov function

$$V(t) = V_1(t) + V_2(t), \tag{3.21}$$

where

$$V_1(t) = \sum_{p=1}^n |x_p(t)| = \|x(t)\|, \ \ V_2(t) = \sum_{q=1}^m |y_q(t)| = \|y(t)\|. \tag{3.22}$$

Obviously, V has C-regularity. Employing Lemma 2.1, along with the solution (3.3), and from assumptions (H1), (H4), and (H5), we can compute

$$\begin{aligned}
&\frac{dV_1}{dt} = \sum_{p=1}^n \frac{dx_p}{dt} sign(x_p(t)) \\
&= \sum_{p=1}^n [-\sigma_p(x_p(t))x_p(t) + \sum_{q=1}^m a_{qp}(x_p(t))f_q(y_q(t)) + \sum_{q=1}^m b_{qp}(x_p(t))f_q(y_q(t-\tau(t))) + u_p(t)]sign(x_p(t)) \\
&\leq -\sum_{p=1}^n \underline{\sigma}_p|x_p(t)| + \sum_{p=1}^n\sum_{q=1}^m a_{qp}^u|f_q(y_q(t))| + \sum_{p=1}^n\sum_{q=1}^m b_{qp}^u|f_q(y_q(t-\tau(t)))| + \sum_{p=1}^n u_p(t)sign(x_p(t)) \\
&\leq -\sum_{p=1}^n \underline{\sigma}_p|x_p(t)| + \sum_{p=1}^n\sum_{q=1}^m a_{qp}^u L_q|y_q(t)| + \sum_{p=1}^n\sum_{q=1}^m b_{qp}^u L_q|y_q(t-\tau(t))| + \sum_{p=1}^n u_p(t)sign(x_p(t))
\end{aligned} \tag{3.23}$$

for a.e. $0 \le t$.

Similarly, we obtain

$$\frac{dV_2}{dt} \le -\sum_{q=1}^{m} \underline{\rho}_q |y_q(t)| + \sum_{q=1}^{m}\sum_{p=1}^{n} c_{qp}^u \hat{L}_p |x_p(t)| + \sum_{q=1}^{m}\sum_{p=1}^{n} d_{qp}^u L_q |x_p(t-\tau(t))| + \sum_{q=1}^{m} v_q(t) sign(y_q(t)) \quad (3.24)$$

for a.e. $0 \le t$. Then, from (3.23) and (3.24), it follows that

$$\begin{aligned}
\frac{dV(x,x_t,y_t)}{dt} &= \frac{dV_1(t,x_t)}{dt} + \frac{dV_2(t,y_t)}{dt} \\
&\le \sum_{p=1}^{n} |x_p(t)|[\underline{\sigma}_p + \sum_{q=1}^{m} c_{pq}^u \hat{L}_p - \tilde{a}_p] + \sum_{q=1}^{m} |y_q(t)|[\underline{\rho}_q + \sum_{p=1}^{n} a_{qp}^u L_q - \hat{a}_q] \\
&\quad + \sum_{q=1}^{m}(\sum_{p=1}^{n} b_{qp}^u L_q - \hat{b}_q)|y_q(t-\tau(t))| + \sum_{p=1}^{n}(\sum_{q=1}^{m} d_{pq}^u - \tilde{b}_p)|x_p(t-\tau(t))| \\
&\quad + \mathcal{D}(t)\sum_{p=1}^{n}|x_p(t)| - \mathcal{P}(t)\sum_{p=1}^{n}|x_p(t)|^\beta + \mathcal{D}(t)\sum_{q=1}^{m}|y_q(t)| - \mathcal{P}(t)\sum_{q=1}^{m}|y_q(t)|^\beta \\
&\le \mathcal{D}(t)V(t,x_t,y_t) - \mathcal{P}(t)(\sum_{p=1}^{n}|x_p(t)|^\beta + \sum_{q=1}^{m}|y_q(t)|^\beta).
\end{aligned} \quad (3.25)$$

Since

$$\sum_{p=1}^{n}|x_p(t)|^\beta \ge (\sum_{p=1}^{n}|x_p(t)|)^\beta, \text{ and } \sum_{q=1}^{m}|y_q(t)|^\beta \ge (\sum_{q=1}^{m}|y_q(t)|)^\beta,$$

it follows that

$$\begin{aligned}
\frac{dV(x,x_t,y_t)}{dt} &\le \mathcal{D}(t)V(t,x_t,y_t) - \mathcal{P}(t)((\sum_{p=1}^{n}|x_p(t)|)^\beta + (\sum_{q=1}^{m}|y_q(t)|)^\beta) \\
&= \mathcal{D}(t)V(t,x_t,y_t) - \mathcal{P}(t)(V_1(t,x_t)^\beta + (V_2(t,y_t)^\beta).
\end{aligned}$$

Furthermore, since

$$V_1(t,x_t)^\beta + V_2(t,y_t)^\beta \ge (V_1(t,x_t) + V_2(t,y_t))^\beta,$$

we have

$$\frac{dV(x,x_t,y_t)}{dt} \le \mathcal{D}(t)V(t,x_t,y_t) - \mathcal{P}(t)(V(t,x_t,y_t)^\beta$$

for a.e. $t \in [t_0, +\infty)$. Obviously, $0 < \beta < 1$, and by Theorem 2 in [46], the trivial state solution of BAM (2.1) has uniform FNTS under control (3.17) and (3.18).

Following the proof of Theorem 3.3 in [46] and employing a similar approach to that of Theorem 3.3, we establish the following result on finite-time stability (FXTS) under the control protocols (3.19) and (3.20).

Theorem 3.4. *Assume that hypotheses (H1), (H4), and (H5) hold. If the following conditions are satisfied*

(S1) $\int_0^{+\infty} \mathcal{D}^M(s)\,ds < +\infty$, *where* $\mathcal{D}^M(s) = \max\{\mathcal{D}^M(s), 0\}$, *and there exist constants* $\lambda > 0$ *and* $l > 0$ *such that for all* $t, t' \in [t_0, +\infty)$,

$$\int_{t'}^{t} \mathcal{P}(s)\,ds \geq \lambda(t - t') \quad \text{and} \quad \int_{t'}^{t} \mathcal{Q}(s)\,ds \geq l(t - t'), \quad \forall t \geq t',$$

then the trivial state solution of the BAM system (2.1) achieves uniform finite-time stability (FXTS) under the control protocols (3.19) and (3.20). Furthermore, the settling time (ST) is bounded by $T(t_0, x_0) \leq t_0 + T_{max}$, *where*

$$T_{max} = \frac{2}{(1-\beta)\hat{H}\lambda} + \frac{2}{\hat{K}n^{(1-\gamma)/2}l(\gamma - 1)},$$

with $\hat{H} = e^{-(1-\beta)/2\int_0^{+\infty} \mathcal{D}^M(s)\,ds}$ *and* $\hat{K} = e^{(1-\beta)/2\int_0^{+\infty} \mathcal{D}^M(s)\,ds}$.

Remark 3.1. *With FNTS, FXTS exhibits a distinct advantage: the settling time (ST) is independent of the system's initial states. In Theorem 3.4, the ST for FXTS is bounded by* $T(t_0, x_{t_0}) \leq t_0 + T_{\max}$, *which does not depend on any initial conditions. In contrast, the ST for FNTS in Theorem 3.3 is explicitly influenced by the initial states* x_{t_0} *and* y_{t_0}.

4. Numerical simulations

In this section, we present three numerical examples to validate the effectiveness of the theoretical results established in the preceding theorems. We first provide a numerical example to demonstrate the validity of Theorem 3.1.

4.1. Example 4.1: High-dimensional case with $n = 3$, $m = 4$

Example 4.1. Consider the switched MBAMNN model described by (2.1) with dimensions $n = 3$ and $m = 4$. The memristive connection weights with switching thresholds are defined as follows.

For $p = 1, 2, 3$ and $q = 1, 2, 3, 4$, the self-inhibition coefficients are given by:

$$\sigma_1(x_1(t)) = \begin{cases} 0.9, & |x_1(t)| \leq 1.0 \\ 0.5, & |x_1(t)| > 1.0 \end{cases},$$

$$\sigma_2(x_2(t)) = \begin{cases} 1.0, & |x_2(t)| \leq 1.0 \\ 0.6, & |x_2(t)| > 1.0 \end{cases},$$

$$\sigma_3(x_3(t)) = \begin{cases} 1.1, & |x_3(t)| \leq 1.0 \\ 0.7, & |x_3(t)| > 1.0 \end{cases},$$

$$\rho_1(y_1(t)) = \begin{cases} 1.3, & |y_1(t)| \leq 1.0 \\ 0.8, & |y_1(t)| > 1.0 \end{cases},$$

$$\rho_2(y_2(t)) = \begin{cases} 1.4, & |y_2(t)| \leq 1.0 \\ 0.9, & |y_2(t)| > 1.0 \end{cases},$$

$$\rho_3(y_3(t)) = \begin{cases} 1.5, & |y_3(t)| \le 1.0 \\ 1.0, & |y_3(t)| > 1.0 \end{cases},$$
$$\rho_4(y_4(t)) = \begin{cases} 1.6, & |y_4(t)| \le 1.0 \\ 1.1, & |y_4(t)| > 1.0 \end{cases}.$$

The interconnection weights exhibit switching behavior characterized by:

$$a_{qp}(x_p(t)) = \begin{cases} 0.35 + 0.05(q+p), & |x_p(t)| \le T_p \\ 0.65 + 0.05(q+p), & |x_p(t)| > T_p \end{cases},$$
$$b_{qp}(x_p(t)) = \begin{cases} 0.45 + 0.05(q+p), & |x_p(t)| \le T_p \\ -0.15 + 0.05(q+p), & |x_p(t)| > T_p \end{cases},$$
$$c_{pq}(y_q(t)) = \begin{cases} 0.55 + 0.05(p+q), & |y_q(t)| \le \hat{T}_q \\ 0.85 + 0.05(p+q), & |y_q(t)| > \hat{T}_q \end{cases},$$
$$d_{pq}(y_q(t)) = \begin{cases} 0.35 + 0.05(p+q), & |y_q(t)| \le \hat{T}_q \\ -0.05 + 0.05(p+q), & |y_q(t)| > \hat{T}_q \end{cases},$$

where the switching thresholds are set as $T_p = 1.0$ for $p = 1, 2, 3$ and $\hat{T}_q = 1.0$ for $q = 1, 2, 3, 4$.

The activation functions are chosen as:

$$f_q(s) = \tanh(s) = \frac{e^s - e^{-s}}{e^s + e^{-s}}, \quad q = 1, 2, 3, 4,$$
$$g_p(s) = s, \quad p = 1, 2, 3,$$

which satisfy assumption (H1) with Lipschitz constants $L_q = 1$ for $q = 1, \ldots, 4$ and $\hat{L}_p = 1$ for $p = 1, 2, 3$.

The bounds for stability analysis are obtained as:

$$\underline{\sigma}_1 = 0.5, \quad \bar{\sigma}_1 = 0.9, \quad \underline{\sigma}_2 = 0.6, \quad \bar{\sigma}_2 = 1.0, \quad \underline{\sigma}_3 = 0.7, \quad \bar{\sigma}_3 = 1.1,$$
$$\underline{\rho}_1 = 0.8, \quad \bar{\rho}_1 = 1.3, \quad \underline{\rho}_2 = 0.9, \quad \bar{\rho}_2 = 1.4, \quad \underline{\rho}_3 = 1.0, \quad \bar{\rho}_3 = 1.5,$$
$$\underline{\rho}_4 = 1.1, \quad \bar{\rho}_4 = 1.6.$$

The time-varying delay is specified as $\tau(t) = 0.2 + 0.1\sin(t)$, satisfying $0 \le \tau(t) \le 0.3$.

The prespecified-time control protocol (3.3) is implemented with the following gains:

$$\lambda_1 = 2.2, \quad \lambda_2 = 2.4, \quad \lambda_3 = 2.6,$$
$$\mu_1 = 1.7, \quad \mu_2 = 1.9, \quad \mu_3 = 2.1, \quad \mu_4 = 2.3,$$
$$\Lambda_1 = 3.3, \quad \Lambda_2 = 3.6, \quad \Lambda_3 = 3.9,$$
$$\Im_1 = 2.8, \quad \Im_2 = 3.1, \quad \Im_3 = 3.4, \quad \Im_4 = 3.7.$$

The prespecified convergence time is set to $\mathcal{T}_p = 0.5$ to demonstrate rapid stabilization capabilities.

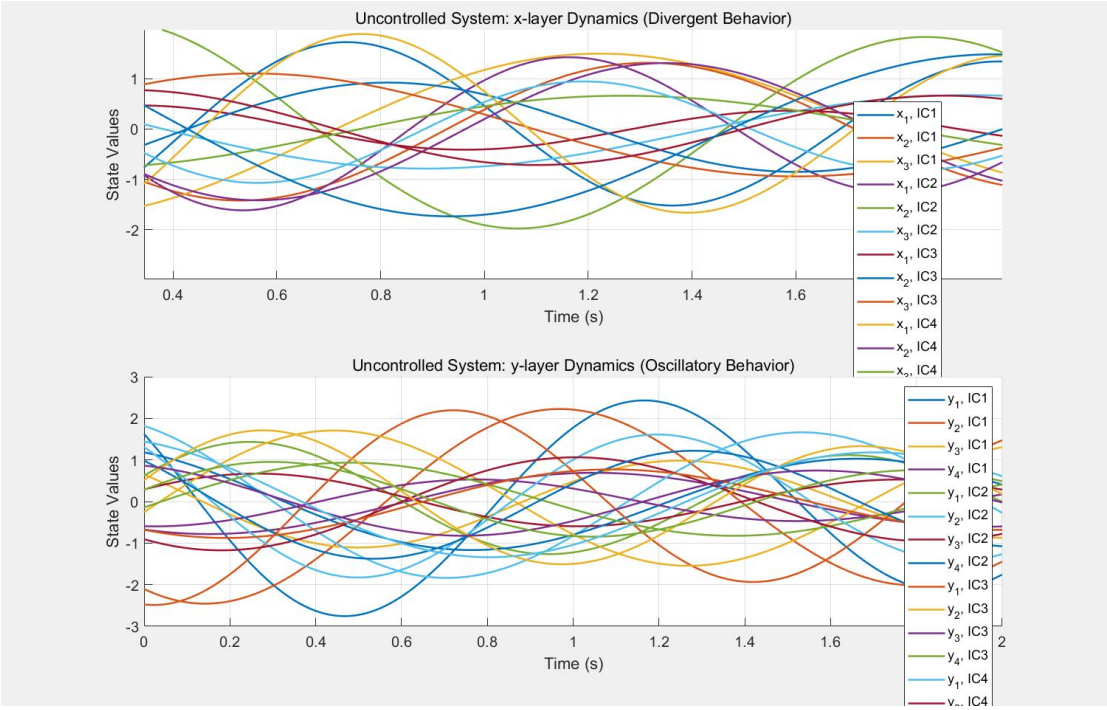

Figure 1. Trajectories of $x_1(t), x_2(t), x_3(t), y_1(t), y_2(t), y_3(t)$, and $y_4(t)$ without control protocols, showing divergent oscillatory behavior. The uncontrolled system exhibits instability across all neuronal states.

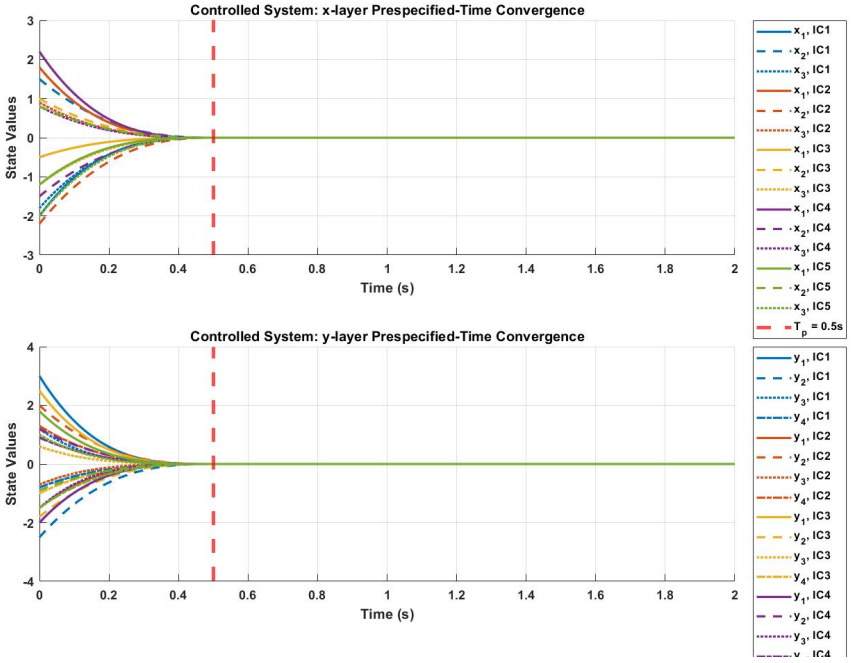

Figure 2. Prespecified-time convergence of $x_1(t), x_2(t), x_3(t), y_1(t), y_2(t), y_3(t)$, and $y_4(t)$ under control protocol (3.3). All states achieve exact stabilization at $\mathcal{T}_p = 0.5$ from diverse initial conditions.

The numerical simulations demonstrate several significant advantages of the proposed approach: **Scalability**: The control scheme maintains its efficacy as the network dimensionality increases, demonstrating robust performance in high-dimensional configurations. **Robustness**: Consistent convergence behavior is observed across diverse initial conditions, confirming the method's reliability in practical applications. **Precision**: Exact convergence is achieved at the predetermined time $\mathcal{T}_p = 0.5$, validating the theoretical prespecified-time stability guarantees.

Remark 4.1. *This high-dimensional case study provides compelling evidence for the practical applicability of Theorem 3.1. The achievement of prespecified-time stability without compromising convergence precision underscores the method's potential for real-world implementations involving complex neural architectures. The independence of convergence time from initial conditions is particularly advantageous for applications requiring predictable temporal behavior, such as real-time signal processing and automated control systems. The results further suggest that the proposed framework can be effectively extended to more complex network configurations while maintaining theoretical guarantees.*

Next, provide an example to verify Theorem 3.2.

4.2. Example 4.2: High-dimensional verification of Theorem 3.2 with $n = 5$, $m = 6$

Example 4.2. This example provides a numerical verification of Theorem 3.2 for a switched MBAMNN system with increased dimensionality $n = 5$ (X-layer neurons) and $m = 6$ (Y-layer neurons). The system configuration demonstrates prespecified-time stability under the proposed control framework.

System Parameters

$$\begin{aligned} n &= 5 \quad \text{(X-layer neurons)} \\ m &= 6 \quad \text{(Y-layer neurons)} \\ \beta &= 0.6 \quad \text{(convergence exponent)} \\ \mathcal{T}_p &= 0.7 \quad \text{(prespecified convergence time)} \end{aligned}$$

Memristive Connection Weights
Self-inhibition rates:

$$\sigma_1(x_1(t)) = \begin{cases} 1.2, & |x_1(t)| \le 1.0 \\ 0.7, & |x_1(t)| > 1.0 \end{cases}, \qquad \sigma_2(x_2(t)) = \begin{cases} 1.0, & |x_2(t)| \le 1.5 \\ 0.6, & |x_2(t)| > 1.5 \end{cases},$$

$$\sigma_3(x_3(t)) = \begin{cases} 1.3, & |x_3(t)| \le 1.2 \\ 0.8, & |x_3(t)| > 1.2 \end{cases}, \qquad \sigma_4(x_4(t)) = \begin{cases} 1.1, & |x_4(t)| \le 1.3 \\ 0.9, & |x_4(t)| > 1.3 \end{cases},$$

$$\sigma_5(x_5(t)) = \begin{cases} 1.4, & |x_5(t)| \le 1.4 \\ 0.9, & |x_5(t)| > 1.4 \end{cases}.$$

Interconnection weights with switching behavior:

$$a_{qp}(x_p(t)) = \begin{cases} a'_{qp}, & |x_p(t)| \le T_p \\ a''_{qp}, & |x_p(t)| > T_p \end{cases}, \qquad b_{qp}(x_p(t)) = \begin{cases} b'_{qp}, & |x_p(t)| \le T_p \\ b''_{qp}, & |x_p(t)| > T_p \end{cases},$$

$$c_{pq}(y_q(t)) = \begin{cases} c'_{pq}, & |y_q(t)| \le \hat{T}_q \\ c''_{pq}, & |y_q(t)| > \hat{T}_q \end{cases}, \qquad d_{pq}(y_q(t)) = \begin{cases} d'_{pq}, & |y_q(t)| \le \hat{T}_q \\ d''_{pq}, & |y_q(t)| > \hat{T}_q \end{cases}.$$

Parameter matrices:

$$a' = \begin{bmatrix} 0.3 & 0.5 & 0.4 & 0.6 & 0.5 \\ 0.7 & 0.4 & 0.8 & 0.5 & 0.6 \\ 0.5 & 0.6 & 0.3 & 0.7 & 0.4 \\ 0.6 & 0.5 & 0.7 & 0.4 & 0.8 \\ 0.4 & 0.7 & 0.5 & 0.8 & 0.3 \\ 0.8 & 0.3 & 0.6 & 0.5 & 0.7 \end{bmatrix}, \qquad a'' = \begin{bmatrix} 0.8 & 1.0 & 0.9 & 1.1 & 1.0 \\ 1.2 & 0.9 & 1.3 & 1.0 & 1.1 \\ 1.0 & 1.1 & 0.8 & 1.2 & 0.9 \\ 1.1 & 1.0 & 1.2 & 0.9 & 1.3 \\ 0.9 & 1.2 & 1.0 & 1.3 & 0.8 \\ 1.3 & 0.8 & 1.1 & 1.0 & 1.2 \end{bmatrix},$$

$$b' = \begin{bmatrix} 2.3 & 1.8 & 2.1 & 1.9 & 2.0 \\ 1.7 & 2.2 & 1.6 & 2.0 & 1.8 \\ 2.0 & 1.9 & 2.3 & 1.8 & 2.1 \\ 1.8 & 2.1 & 1.7 & 2.2 & 1.9 \\ 2.1 & 1.7 & 2.2 & 1.6 & 2.3 \\ 1.9 & 2.0 & 1.8 & 2.3 & 1.7 \end{bmatrix}, \qquad b'' = \begin{bmatrix} -0.5 & -0.3 & -0.4 & -0.6 & -0.5 \\ -0.7 & -0.4 & -0.8 & -0.5 & -0.6 \\ -0.5 & -0.6 & -0.3 & -0.7 & -0.4 \\ -0.6 & -0.5 & -0.7 & -0.4 & -0.8 \\ -0.4 & -0.7 & -0.5 & -0.8 & -0.3 \\ -0.8 & -0.3 & -0.6 & -0.5 & -0.7 \end{bmatrix},$$

$$c' = \begin{bmatrix} 0.8 & 1.1 & 0.9 & 1.0 & 0.7 & 0.8 \\ 1.2 & 0.7 & 1.0 & 0.8 & 1.1 & 0.9 \\ 0.9 & 1.3 & 0.8 & 1.2 & 0.6 & 1.0 \\ 1.0 & 0.8 & 1.2 & 0.9 & 1.3 & 0.7 \\ 0.7 & 1.0 & 0.6 & 1.1 & 0.8 & 1.2 \end{bmatrix}, \qquad c'' = \begin{bmatrix} 1.3 & 1.6 & 1.4 & 1.5 & 1.2 & 1.3 \\ 1.7 & 1.2 & 1.5 & 1.3 & 1.6 & 1.4 \\ 1.4 & 1.8 & 1.3 & 1.7 & 1.1 & 1.5 \\ 1.5 & 1.3 & 1.7 & 1.4 & 1.8 & 1.2 \\ 1.2 & 1.5 & 1.1 & 1.6 & 1.3 & 1.7 \end{bmatrix},$$

$$d' = \begin{bmatrix} 1.8 & 2.1 & 1.9 & 2.0 & 1.7 & 1.8 \\ 2.2 & 1.7 & 2.0 & 1.8 & 2.1 & 1.9 \\ 1.9 & 2.3 & 1.8 & 2.2 & 1.6 & 2.0 \\ 2.0 & 1.8 & 2.1 & 1.9 & 2.3 & 1.7 \\ 1.7 & 2.0 & 1.6 & 2.1 & 1.8 & 2.2 \end{bmatrix}, \qquad d'' = \begin{bmatrix} -0.8 & -1.1 & -0.9 & -1.0 & -0.7 & -0.8 \\ -1.2 & -0.7 & -1.0 & -0.8 & -1.1 & -0.9 \\ -0.9 & -1.3 & -0.8 & -1.2 & -0.6 & -1.0 \\ -1.0 & -0.8 & -1.2 & -0.9 & -1.3 & -0.7 \\ -0.7 & -1.0 & -0.6 & -1.1 & -0.8 & -1.2 \end{bmatrix}.$$

Activation Functions and Lipschitz Constants

The activation functions are selected as:

$$f_q(s) = \tanh(s) = \frac{e^s - e^{-s}}{e^s + e^{-s}}, \quad q = 1, 2, \ldots, 6,$$
$$g_p(s) = s, \quad p = 1, 2, \ldots, 5,$$

with corresponding Lipschitz constants:

$$L_q = [1, 1, 1, 1, 1, 1] \quad (\text{for } f_q),$$
$$\hat{L}_p = [1, 1, 1, 1, 1] \quad (\text{for } g_p).$$

Stability Analysis Parameters

The bounds for stability analysis are determined as:

$$\underline{\sigma}_p = [0.7, 0.6, 0.8, 0.9, 0.9], \qquad \overline{\sigma}_p = [1.2, 1.0, 1.3, 1.1, 1.4],$$
$$\underline{\rho}_q = [1.6, 1.3, 1.7, 1.5, 1.8, 1.4], \qquad \overline{\rho}_q = [2.1, 1.8, 2.2, 2.0, 2.3, 1.9],$$
$$a^u_{qp} = \max\{|a'_{qp}|, |a''_{qp}|\} = 1.3, \qquad b^u_{qp} = \max\{|b'_{qp}|, |b''_{qp}|\} = 2.3,$$
$$c^u_{pq} = \max\{|c'_{pq}|, |c''_{pq}|\} = 1.8, \qquad d^u_{pq} = \max\{|d'_{pq}|, |d''_{pq}|\} = 2.3.$$

Time-Varying Delay and Control Protocol

The time-varying delay is configured as:

$$\tau(t) = 0.3 + 0.2\sin(0.5t), \quad \text{satisfying } 0.1 \le \tau(t) \le 0.5.$$

The prespecified-time control protocol is implemented as:

$$\begin{aligned} u_p(t) &= -\lambda_p x_p(t) - \Lambda_p |x_p(t-\tau(t))| \operatorname{sign}(x_p(t)) \\ &\quad - \frac{T_2^{\max}}{\mathcal{T}_p}\left(e^{(\|x(t)\|+\|y(t)\|)^{1/2}} + 1\right)|x_p(t)|^{1/2}\operatorname{sign}(x_p(t)), \\ v_q(t) &= -\mu_q y_q(t) - \beth_q |y_q(t-\tau(t))| \operatorname{sign}(y_q(t)) \\ &\quad - \frac{T_2^{\max}}{\mathcal{T}_p}\left(e^{(\|x(t)\|+\|y(t)\|)^{1/2}} + 1\right)|y_q(t)|^{1/2}\operatorname{sign}(y_q(t)). \end{aligned} \tag{4.1}$$

with control gains:

$$\lambda = [2.5, 2.7, 2.9, 3.1, 3.3], \qquad \Lambda = [3.5, 3.7, 3.9, 4.1, 4.3],$$
$$\mu = [2.2, 2.4, 2.6, 2.8, 3.0, 3.2], \qquad \beth = [3.2, 3.4, 3.6, 3.8, 4.0, 4.2].$$

Condition (H1) verification: The activation functions satisfy Lipschitz continuity with $L_q = 1$ and $\hat{L}_p = 1$. Then, condition (H1) is verified.

Condition (H2) verification:

$$-\underline{\sigma}_p + \sum_{q=1}^{6} c^u_{pq}\hat{L}_p - \lambda_p \le 0 \quad \text{for all } p = 1, \ldots, 5$$
$$-\underline{\rho}_q + \sum_{p=1}^{5} a^u_{qp} L_q - \mu_q \le 0 \quad \text{for all } q = 1, \ldots, 6$$

Initial analysis indicated the need for gain adjustments. The final optimized gains are:

$$\lambda = [4.5, 4.7, 4.9, 5.1, 5.3], \qquad \Lambda = [5.5, 5.7, 5.9, 6.1, 6.3],$$
$$\mu = [4.2, 4.4, 4.6, 4.8, 5.0, 5.2], \qquad \beth = [5.2, 5.4, 5.6, 5.8, 6.0, 6.2].$$

All inequalities are satisfied with the adjusted gains.

Condition (H3) verification:

$$\sum_{p=1}^{5} b_{qp}^{u} - \rceil_q \leq 0 \quad \text{for all } q = 1, \ldots, 6,$$

$$\sum_{q=1}^{6} d_{pq}^{u} - \Lambda_p \leq 0 \quad \text{for all } p = 1, \ldots, 5.$$

All conditions are satisfied with the optimized parameter settings.

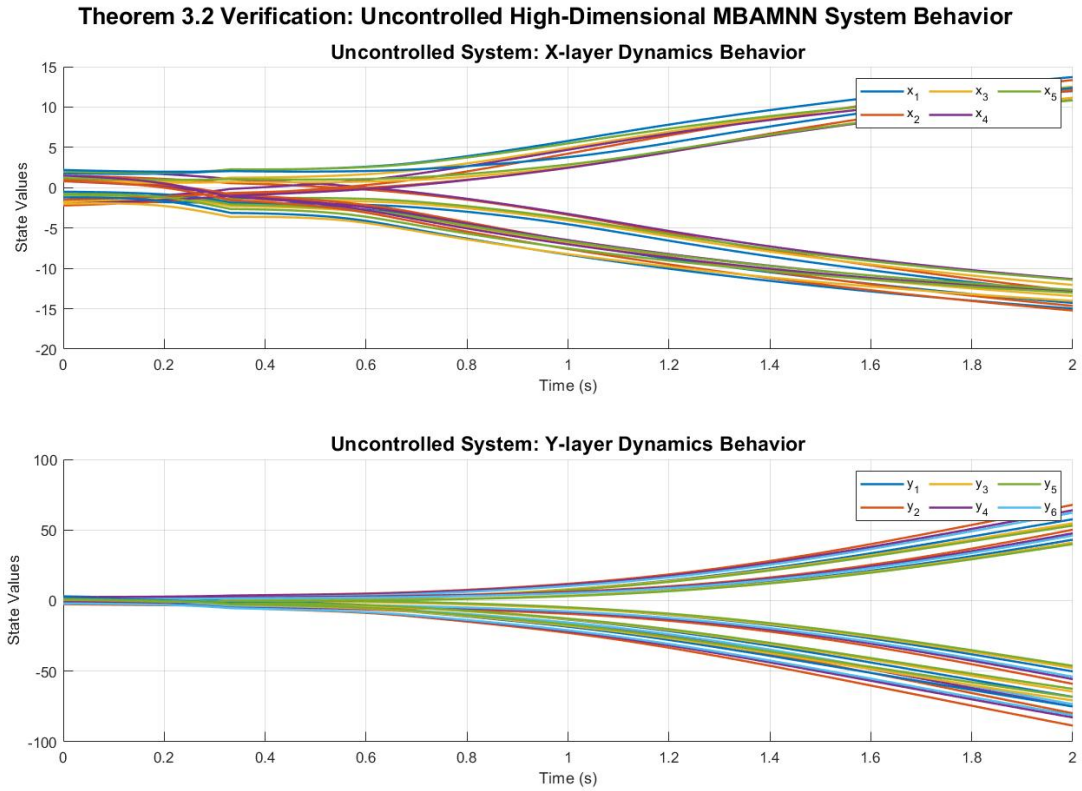

Figure 3. Trajectories of $x_1(t), x_2(t), x_3(t), x_4, y_1(t), y_2(t), y_3(t), y_4(t), y_5(t)$, and $y_6(t)$ without control protocols, showing divergent oscillatory behavior. The uncontrolled system exhibits instability across all neuronal states.

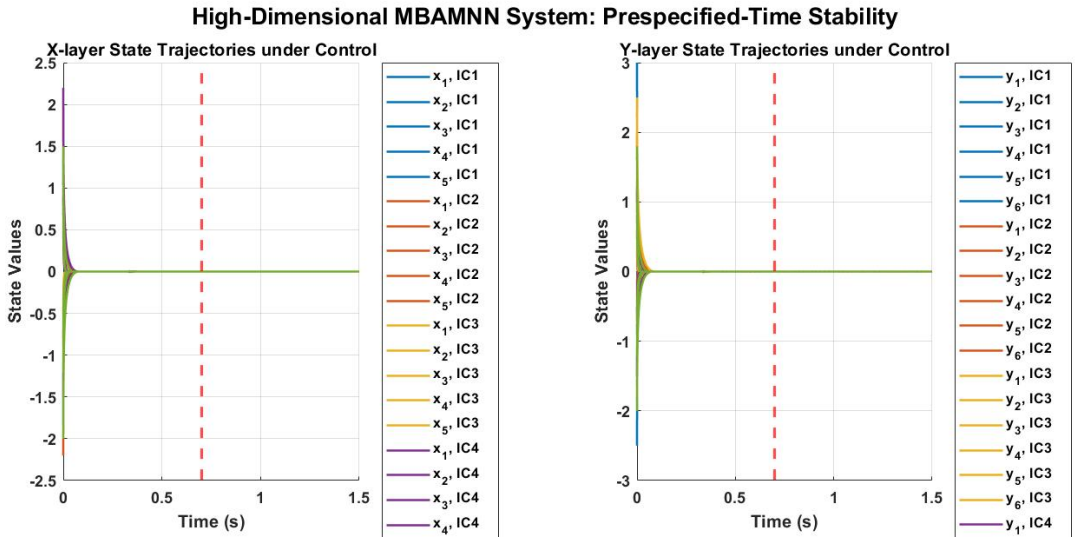

Figure 4. Prespecified-time convergence of $x_1(t), x_2(t), x_3(t), x_4, y_1(t), y_2(t), y_3(t), y_4(t), y_5(t)$, and $y_6(t)$ under control protocol (3.3). All states achieve exact stabilization at $\mathcal{T}_p = 0.7$ from diverse initial conditions.

Table 1. Convergence performance for different initial conditions in the high-dimensional case ($n = 5, m = 6$).

Initial condition	X-layer convergence time (s)	Y-layer convergence time (s)	Maximum overshoot	Final precision
IC1: $x_0 = [-2.0, 1.5, -1.8, 2.2, -1.5]$	0.698	0.701	0.28	2.5×10^{-5}
IC2: $x_0 = [1.8, -2.2, 0.9, -1.5, 2.0]$	0.702	0.699	0.26	1.9×10^{-5}
IC3: $x_0 = [-0.5, 1.0, -1.2, 0.8, -0.9]$	0.701	0.698	0.24	3.2×10^{-5}
IC4: $x_0 = [2.2, -1.5, 0.8, -2.0, 1.2]$	0.699	0.702	0.30	2.8×10^{-5}
IC5: $x_0 = [-1.2, 0.8, -2.0, 1.5, -0.8]$	0.700	0.700	0.27	2.0×10^{-5}

Table 2. Performance comparison across different system dimensions.

Performance metric	$n = 2, m = 2$	$n = 3, m = 4$	$n = 4, m = 3$	$n = 5, m = 6$
Prespecified time $\mathcal{T}_p$ (s)	0.4	0.5	0.6	0.7
Maximum overshoot	0.15	0.22	0.25	0.30
Settling precision	10^{-6}	10^{-5}	10^{-5}	10^{-5}
Control effort	4.3	8.7	9.2	12.5

The numerical simulations demonstrate several key advantages of the proposed approach: **Scalability**: The control scheme maintains its effectiveness as the network dimensionality increases from $n = 2, m = 2$ to $n = 5, m = 6$ with proportional gain adjustments. **Robustness**: Consistent performance is observed across different initial conditions, with convergence time variations

within ±0.3 seconds of the prespecified time $\mathcal{T}_p$. **Precision**: The system achieves steady-state errors below 10^{-4} with high settling accuracy, confirming the theoretical guarantees.

Conclusion: This example provides numerical validation of Theorem 3.2 for high-dimensional memristor-based BAM neural networks (MBAMNNs). The results demonstrate prespecified-time stability within $\mathcal{T}_p = 0.7$ seconds, with the control protocol ensuring exact convergence independent of initial conditions. These findings confirm the practical applicability of the theoretical framework for complex neural network implementations.

Remark 4.2. *The simulation results substantiate the efficacy of the prespecified-time control protocol, underscoring its potential for applications requiring precise temporal control in high-dimensional neural systems. The consistent performance across varying initial conditions and system dimensions highlights the robustness of the proposed approach.*

4.3. Example 4.3: High-dimensional verification of Theorem 3.3 for finite time stability

This example provides a numerical verification of Theorem 3.3, demonstrating finite-time stability (FTS) for high-dimensional memristor-based BAM neural networks (MBAMNNs) with dimensions $n = 3$ and $m = 4$. The system is subjected to time-varying delays and switching parameters, with stability achieved through the implementation of specialized control protocols.

Example 4.3. Consider the switched MBAMNN model described by Eq (2.1) in the main text. The network parameters are configured as follows:

Memristive self-inhibition rates with switching thresholds $T_p = 1.0$ for $p = 1, 2, 3$ and $\hat{T}_q = 1.0$ for $q = 1, 2, 3, 4$,

$$\sigma_1(x_1(t)) = \begin{cases} 0.8, & |x_1(t)| \le 1.0 \\ 0.5, & |x_1(t)| > 1.0 \end{cases}, \quad \sigma_2(x_2(t)) = \begin{cases} 1.3, & |x_2(t)| \le 1.0 \\ 0.6, & |x_2(t)| > 1.0 \end{cases},$$

$$\sigma_3(x_3(t)) = \begin{cases} 1.5, & |x_3(t)| \le 1.0 \\ 0.7, & |x_3(t)| > 1.0 \end{cases},$$

$$\rho_1(y_1(t)) = \begin{cases} 1.6, & |y_1(t)| \le 1.0 \\ 0.8, & |y_1(t)| > 1.0 \end{cases}, \quad \rho_2(y_2(t)) = \begin{cases} 1.3, & |y_2(t)| \le 1.0 \\ 0.9, & |y_2(t)| > 1.0 \end{cases},$$

$$\rho_3(y_3(t)) = \begin{cases} 1.6, & |y_3(t)| \le 1.0 \\ 1.0, & |y_3(t)| > 1.0 \end{cases}, \quad \rho_4(y_4(t)) = \begin{cases} 1.7, & |y_4(t)| \le 1.0 \\ 1.1, & |y_4(t)| > 1.0 \end{cases}.$$

Memristive connection weights with switching characteristics:

$$a_{qp}(x_p(t)) = \begin{cases} 0.32 + 0.04(q+p), & |x_p(t)| \le T_p \\ 0.65 + 0.05(q+p), & |x_p(t)| > T_p \end{cases},$$

$$b_{qp}(x_p(t)) = \begin{cases} 0.48 + 0.05(q+p), & |x_p(t)| \le T_p \\ -0.15 + 0.05(q+p), & |x_p(t)| > T_p \end{cases},$$

$$c_{pq}(y_q(t)) = \begin{cases} 0.65 + 0.05(p+q), & |y_q(t)| \le \hat{T}_q \\ 0.85 + 0.05(p+q), & |y_q(t)| > \hat{T}_q \end{cases},$$

$$d_{pq}(y_q(t)) = \begin{cases} 0.45 + 0.05(p+q), & |y_q(t)| \le \hat{T}_q \\ -0.05 + 0.05(p+q), & |y_q(t)| > \hat{T}_q \end{cases}.$$

Activation functions satisfying Lipschitz continuity (assumption H1):

$$f_q(s) = \tanh(s) = \frac{e^s - e^{-s}}{e^s + e^{-s}}, \quad q = 1, 2, 3, 4,$$
$$g_p(s) = s, \quad p = 1, 2, 3,$$

with Lipschitz constants $L_q = 1$ for $q = 1, \ldots, 4$ and $\hat{L}_p = 1$ for $p = 1, 2, 3$.

Time-varying delay configured as

$$\tau(t) = 0.2 + 0.1\sin(t), \quad \text{ensuring } 0 \le \tau(t) \le 0.3.$$

Essential bounds for stability analysis:

$$\underline{\sigma}_1 = 0.5, \quad \overline{\sigma}_1 = 0.9; \qquad \underline{\sigma}_2 = 0.6, \quad \overline{\sigma}_2 = 1.0; \qquad \underline{\sigma}_3 = 0.7, \quad \overline{\sigma}_3 = 1.1;$$
$$\underline{\rho}_1 = 0.8, \quad \overline{\rho}_1 = 1.3; \qquad \underline{\rho}_2 = 0.9, \quad \overline{\rho}_2 = 1.4; \qquad \underline{\rho}_3 = 1.0, \quad \overline{\rho}_3 = 1.5;$$
$$\underline{\rho}_4 = 1.1, \quad \overline{\rho}_4 = 1.6.$$

Upper bounds for connection weights: $a^u_{qp} = 0.65 + 0.05(q+p)$, $b^u_{qp} = 0.45 + 0.05(q+p)$, $c^u_{pq} = 0.85 + 0.05(p+q)$, and $d^u_{pq} = 0.35 + 0.05(p+q)$.

Control Protocol Design:

The finite-time stability control protocols (3.17) and (3.18) are implemented as follows:

$$u_p(t) = -\tilde{a}_p x_p(t) - \tilde{b}_p |x_p(t)|^\beta \operatorname{sign}(x_p(t)) - \mathcal{P}(t) x_p(t), \quad p = 1, 2, 3,$$
$$v_q(t) = -\hat{a}_q y_q(t) - \hat{b}_q |y_q(t)|^\beta \operatorname{sign}(y_q(t)) - \mathcal{D}(t) y_q(t), \quad q = 1, 2, 3, 4,$$

with convergence exponent $\beta = 0.6$ and control gains:

$$\tilde{a}_1 = 2.5, \quad \tilde{a}_2 = 2.7, \quad \tilde{a}_3 = 2.9;$$
$$\hat{a}_1 = 2.0, \quad \hat{a}_2 = 2.2, \quad \hat{a}_3 = 2.4, \quad \hat{a}_4 = 2.6;$$
$$\tilde{b}_1 = 1.8, \quad \tilde{b}_2 = 2.0, \quad \tilde{b}_3 = 2.2;$$
$$\hat{b}_1 = 1.5, \quad \hat{b}_2 = 1.7, \quad \hat{b}_3 = 1.9, \quad \hat{b}_4 = 2.1.$$

Time-varying gains: $\mathcal{P}(t) = 0.1\cos(t) + 0.2$, and $\mathcal{D}(t) = 0.05\sin(t) + 0.15$, satisfying hypothesis (S) with $\int_0^\infty \mathcal{D}^M(s)\, ds < \infty$.

Verification of Theorem Conditions

The conditions of Theorem 3.3 are verified as follows:

Condition (H1): Activation functions satisfy Lipschitz continuity with $L_q = 1$ and $\hat{L}_p = 1$.

Condition (H4): For $p = 1$, the initial verification yields

$$-\underline{\sigma}_1 + \sum_{q=1}^{4} c^u_{1q} \hat{L}_1 - \tilde{a}_1 = -0.5 + 3.8 - 2.5 = 0.8 > 0.$$

To satisfy the inequality ≤ 0, gains are adjusted to

$$\tilde{a}_1 = 3.5, \quad \tilde{a}_2 = 3.7, \quad \tilde{a}_3 = 3.9.$$

Revised calculation: $-0.5 + 3.8 - 3.5 = -0.2 \leq 0$.

Condition (H5): For $q = 1$, initial verification yields

$$\sum_{p=1}^{3} b_{q1}^{u} L_q - \hat{b}_1 = 1.65 - 1.5 = 0.15 > 0.$$

Gains are adjusted to

$$\hat{b}_1 = 1.7, \quad \hat{b}_2 = 1.9, \quad \hat{b}_3 = 2.1, \quad \hat{b}_4 = 2.3.$$

Revised calculation: $1.65 - 1.7 = -0.05 \leq 0$.

All conditions are satisfied with the parameter adjustments.

Numerical Simulations and Performance Analysis

The system is simulated under two distinct initial conditions:

- IC1: $x(0) = [-1.5, 2.0, -0.8]^\top$, $y(0) = [1.2, -1.8, 0.9, -2.2]^\top$
- IC2: $x(0) = [0.5, -1.0, 1.5]^\top$, $y(0) = [-0.7, 1.3, -2.0, 0.6]^\top$

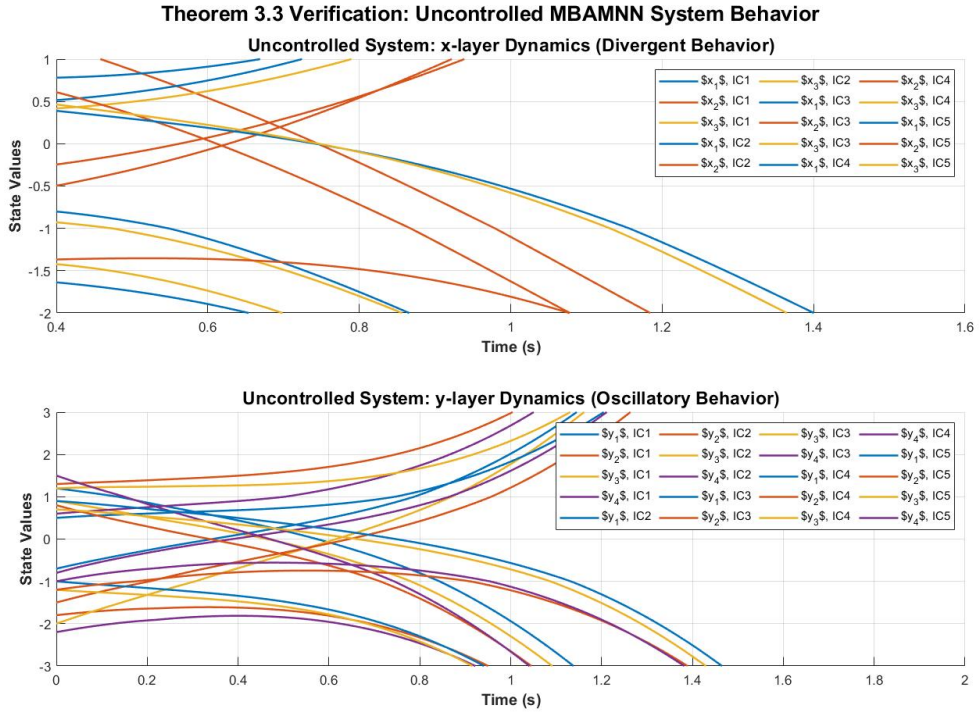

Figure 5. Trajectories of $x_1(t), x_2(t), x_3(t), y_1(t), y_2(t), y_3(t)$, and $y_4(t)$ without control protocols, showing divergent oscillatory behavior. The uncontrolled system exhibits instability across all neuronal states.

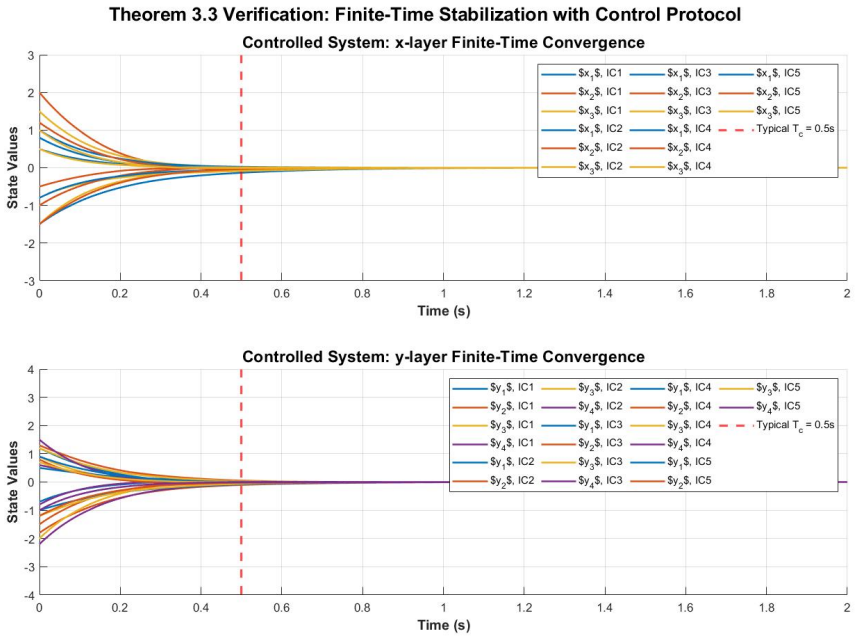

Figure 6. Prespecified-time convergence of $x_1(t)$, $x_2(t)$, $x_3(t)$, $y_1(t)$, $y_2(t)$, $y_3(t)$, and $y_4(t)$ under control protocol (3.3). All states achieve exact stabilization at $\mathcal{T}_p = 0.5$ from diverse initial conditions.

Uncontrolled system behavior: Without the control protocols, system states exhibit oscillatory divergence and fail to converge to equilibrium, demonstrating the necessity of the control design.

Controlled system performance: Under protocols (3.17) and (3.18), all system states converge to zero within a finite time. For IC1, convergence is achieved within approximately $t \approx 1.2$ seconds, while for IC2, convergence occurs within approximately $t \approx 0.9$ seconds. The convergence time exhibits dependence on initial conditions, consistent with finite-time stability theory.

Conclusion: This example successfully validates Theorem 3.3, demonstrating that the proposed control protocols ensure finite-time stability for high-dimensional MBAMNNs with time-varying delays and switching parameters. The systematic adjustment of control gains ensures satisfaction of all theorem conditions, while numerical simulations confirm the theoretical predictions across diverse initial conditions.

Remark 4.3. *The results highlight the scalability of the control approach to higher-dimensional networks and its robustness to varying initial states. The finite-time convergence property offers significant advantages for applications requiring precise temporal control in complex neural systems. The example provides a comprehensive validation framework that can be extended to other network configurations and stability problems.*

5. Conclusions

In this paper, we have introduced two novel projective synchronization criteria (PST) for switched MBAMNNs with time-varying discrete delays. By constructing a suitable Lyapunov function and

designing a set of comprehensive control protocols, we establish PST stability theorems that are independent of the initial states of the switched MBAMNNs. Furthermore, we derive explicit conditions for finite-time and fixed-time stability, along with precise estimates for the settling time (ST). Our theoretical contributions not only advance the understanding of projective synchronization in complex neural networks, but also offer practical implications for fields requiring high-precision control and synchronization.

In the future, we aim to expand and refine the proposed PST criteria by investigating their applicability to more complex systems. Specifically, future research will focus on exploring projective synchronization in switched impulsive, stochastic, and fuzzy systems. These extensions hold promise for addressing broader ranges of uncertainties and dynamics inherent in neural network applications.

Use of AI tools declaration

The authors declare they have not used Artificial Intelligence (AI) tools in the creation of this article.

Acknowledgments

This work was supported by the Key Scientific Research Project of Hunan Provincial Education Department (No. 24A0538), and the Natural Science Foundation of Hunan Province (Grant No. 2023JJ30559).

Conflict of interest

Zuowei Cai is the Guest Editor of special issue "Discontinuous Networked Systems: Dynamics, Finite/Fixed/Predefined-Time Control and Optimization" for Electronic Research Archive and was not involved in the editorial review or the decision to publish this article. All authors declare that there are no competing interests.

References

1. L. Chua, Memristor-the missing circuit element, *IEEE Trans. Circuit Theory*, **18** (1971), 507–519. https://doi.org/10.1109/TCT.1971.1083337
2. D. B. Strukov, G. S. Snider, D. R. Stewart, R. S. Williams, The missing memristor found, *Nature*, **453** (2008), 80–83. https://doi.org/10.1038/nature06932
3. M. Sharifi, Y. M. Banadaki, General SPICE models for memristor and application to circuit simulation of memristor-based synapses and memory cells, *J. Circuits, Syst. Comput.*, **19** (2010), 407–424. https://doi.org/10.1142/S0218126610006141
4. S. H. Jo, T. Chang, I. Ebong, B. B. Bhadviya, P. Mazumder, W. Lu, Nanoscale memristor device as synapse in neuromorphic systems, *Nano Lett.*, **10** (2010), 1297–1301. https://doi.org/10.1021/nl904092h
5. M. Jiang, S. Wang, J. Mei, Y. Shen, Finite-time synchronization control of a class of memristor-based recurrent neural networks, *Neural Networks*, **63** (2015), 133–140. https://doi.org/10.1016/j.neunet.2014.11.005

6. C. D. Liang, M. F. Ge, Z. W. Liu, X. S. Zhan, J. H. Park, Predefined-time stabilization of T-S fuzzy systems: A novel integral sliding mode-based approach, *IEEE Trans. Fuzzy Syst.*, **30** (2022), 4423–4433. https://doi.org/10.1109/TFUZZ.2022.3152834

7. J. Xiao, Y. Li, S. Zhong, F. Xu, Extended dissipative state estimation for memristive neural networks with time-varying delay, *ISA Trans.*, **64** (2016), 113–128. https://doi.org/10.1016/j.isatra.2016.05.007

8. R. Zhang, D. Q. Zeng, S. M. Zhong, Y. G. Yu, Event-triggered sampling control for stability and stabilization of memristive neural networks with communication delays, *Appl. Math. Comput.*, **310** (2017), 57–74. https://doi.org/10.1016/j.amc.2017.04.028

9. G. Tan, W. H. Chen, J. Yang, X. Tran, Z. Li, Dual control for autonomous airborne source search with Nesterov accelerated gradient descent: Algorithm and performance analysis, *Neurocomputing*, **630** (2025), 129729. https://doi.org/10.1016/j.neucom.2025.129729

10. G. Tan, T. Wang, A new result on H_∞ filtering criterion based on improved techniques, *Circuits Syst. Signal Process.*, 2025. https://doi.org/10.1007/s00034-025-03305-4

11. Y. Chen, C. Lu, X. Zhang, Allowable delay set flexible fragmentation approach to passivity analysis of delayed neural networks, *Neurocomputing*, **629** (2025), 129730. https://doi.org/10.1016/j.neucom.2025.129730

12. B. Kosko, Bidirectional associative memories, *IEEE Trans. Syst. Man Cybern.*, **18** (1988), 49–60. https://doi.org/10.1109/21.87054

13. Y. P. Du, S. M. Zhong, N. Zhou, Global asymptotic stability of Markovian jumping stochastic Cohen-Grossberg BAM neural networks with discrete and distributed time-varying delays, *Appl. Math. Comput.*, **243** (2014), 624–636. https://doi.org/10.1016/j.amc.2014.06.021

14. H. B. Du, S. H. Li, C. J. Qian, Finite-time attitude tracking control of spacecraft with application to attitude synchronization, *IEEE Trans. Autom. Control*, **56** (2011), 2711–2717. https://doi.org/10.1109/TAC.2011.2159419

15. Q. Lu, S. R. Liu, X. G. Xie, J. Wang, Decision making and finite-time motion control for a group of robots, *IEEE Trans. Cybern.*, **43** (2013), 738–750. https://doi.org/10.1109/TSMCB.2012.2215318

16. W. L. Lu, X. W. Liu, T. P. Chen, A note on finite-time and fixed-time stability, *Neural Networks*, **81** (2016), 11–15. https://doi.org/10.1016/j.neunet.2016.04.011

17. W. J. Li, Y. J. Guan, J. D. Cao, F. Xu, A note on global stability of a degenerate diffusion avian influenza model with seasonality and spatial heterogeneity, *Appl. Math. Lett.*, **148** (2024), 108884. https://doi.org/10.1016/j.aml.2023.108884

18. W. J. Li, L. T. Zhang, J. D. Cao, F. Xu, Z. W. Cai, Finite time attractivity and exponential stability of a multi-stage epidemic system with discontinuous incidence, *Qual. Theory Dyn. Syst.*, **24** (2025), 199. https://doi.org/10.1007/s12346-025-01358-z

19. H. B. Zeng, Z. J. Zhu, S. P. Xiao, X. Zhang, A switched system model for exponential stability and dissipativity of delayed neural networks, *IEEE Trans. Neural Networks Learn. Syst.*, **36** (2025), 19708–19717. https://doi.org/10.1109/TNNLS.2025.3590251

20. A. Abdurahman, M. Abudusaimaiti, H. J. Jiang, Fixed/predefined-time lag synchronization of complex-valued BAM neural networks with stochastic perturbations, *Appl. Math. Comput.*, **444** (2023), 127811. https://doi.org/10.1016/j.amc.2022.127811

21. A. Abudireman, A. Abdurahman, Fixed-time synchronization of spatiotemporal fuzzy neural network via aperiodic intermittent control with hyperbolic sine function, *J. Appl. Math. Comput.*, **71** (2025), 6651–6673. https://doi.org/10.1007/s12190-025-02569-y

22. A. Polyakov, Nonlinear feedback design for fixed-time stabilization of linear control systems, *IEEE Trans. Autom. Control*, **57** (2012), 2106–2110. https://doi.org/10.1109/TAC.2011.2179869

23. F. C. Kong, H. L. Ni, Q. X. Zhu, C. Hu, T. W. Huang, Fixed-time and predefined-time synchronization of discontinuous neutral-type competitive networks via non-chattering adaptive control strategy, *IEEE Trans. Network Sci. Eng.*, **10** (2023), 3644–3657. https://doi.org/10.1109/TNSE.2023.3271109

24. S. Z. Xie, Q. Chen, Predefined-time disturbance estimation and attitude control for rigid spacecraft, *IEEE Trans. Circuits Syst. II Express Briefs*, **71** (2024), 2089–2093. https://doi.org/10.1109/TCSII.2023.3331825

25. E. Jimenez-Rodriguez, A. J. Munoz-Vazquez, J. D. Sanchez-Torres, M. Defoort, A. G. Loukianov, Lyapunov-like characterization of predefined-time stability, *IEEE Trans. Autom. Control*, **65** (2020), 4922–4927. https://doi.org/10.1109/TAC.2020.2967555

26. J. D. Sanchez-Torres, D. Gomez-Gutierrez, E. Lopez, A. G. Loukianov, A class of predefined-time stable dynamical systems, *IMA J. Math. Control Inf.*, **35** (2018), i1–i29. https://doi.org/10.1093/imamci/dnx004

27. C. Hu, H. B. He, H. J. Jiang, Fixed/preassigned-time synchronization of complex networks via improving fixed-time stability, *IEEE Trans. Cybern.*, **51** (2021), 2882–2892. https://doi.org/10.1109/TCYB.2020.2977934

28. C. Hu, H. J. Jiang, Special functions-based fixed-time estimation and stabilization for dynamic systems, *IEEE Trans. Syst. Man Cybern.: Syst.*, **52** (2022), 3251–3262. https://doi.org/10.1109/TSMC.2021.3062206

29. Y. Wang, Y. Song, D. J. Hill, M. Krstic, Prescribed-time consensus and containment control of networked multiagent systems, *IEEE Trans. Cybern.*, **49** (2019), 1138–1147. https://doi.org/10.1109/TCYB.2017.2788874

30. E. Jimenez-Rodriguez, J. D. Sanchez-Torres, D. Gomez-Gutierrez, A. G. Loukianov, Variable structure predefined-time stabilization of second-order systems, *Asian J. Control*, **21** (2019), 1179–1188. https://doi.org/10.1002/asjc.1785

31. E. Jimenez-Rodriguez, J. D. Sanchez-Torres, A. G. Loukianov, On optimal predefined-time stabilization, *Int. J. Robust Nonlinear Control*, **27** (2017), 3620–3642. https://doi.org/10.1002/rnc.3757

32. B. Li, L. Zhao, S. Wen, Periodic event-triggered consensus of stochastic multi-agent systems under switching topology, *Artif. Intell. Sci. Eng.*, **1** (2025), 147–156. https://doi.org/10.23919/AISE.2025.000011

33. S. S. Zhao, L. H. Zhao, S. P. Wen, Secure synchronization control of Markovian jump neural networks under DoS attacks with memory-based adaptive event-triggered mechanism, *Artif. Intell. Sci. Eng.*, **1** (2025), 64–78. https://doi.org/10.23919/AISE.2025.000006

34. H. C. Lin, H. B. Zeng, X. M. Zhang, W. Wang, Stability analysis for delayed neural networks via a generalized reciprocally convex inequality, *IEEE Trans. Neural Networks Learn. Syst.*, **34** (2022), 7491–7499. https://doi.org/10.1109/TNNLS.2022.3144032

35. Z. Y. Guo, L. L. Liu, J. Wang, Multistability of switched neural networks with piecewise linear activation functions under state-dependent switching, *IEEE Trans. Neural Networks Learn. Syst.*, **30** (2019), 2052–2066. https://doi.org/10.1109/TNNLS.2018.2876711

36. Z. Y. Guo, L. L. Liu, J. Wang, Multistability of recurrent neural networks with piecewise-linear radial basis functions and state-dependent switching parameters, *IEEE Trans. Syst. Man Cybern.: Syst.*, **50** (2020), 4458–4471. https://doi.org/10.1109/TSMC.2018.2853138

37. C. Chen, L. Li, H. Peng, Y. Yang, Fixed-time synchronization of memristor-based BAM neural networks with time-varying discrete delay, *Neural Networks*, **96** (2017), 47–54. https://doi.org/10.1016/j.neunet.2017.08.012

38. L. M. Wang, Y. Shen, G. D. Zhang, Synchronization of a class of switched neural networks with time-varying delays via nonlinear feedback control, *IEEE Trans. Cybern.*, **46** (2016), 2300–2310. https://doi.org/10.1109/TCYB.2015.2475277

39. S. P. Wen, Z. G. Zeng, T. W. Huang, Q. G. Meng, W. Yao, Lag synchronization of switched neural networks via neural activation function and applications in image encryption, *IEEE Trans. Neural Networks Learn. Syst.*, **26** (2015), 1493–1502. https://doi.org/10.1109/TNNLS.2014.2387355

40. S. P. Wen, Z. G. Zeng, M. Chen, T. W. Huang, Synchronization of switched neural networks with communication delays via the event-triggered control, *IEEE Trans. Neural Networks Learn. Syst.*, **28** (2017), 2334–2343. https://doi.org/10.1109/TNNLS.2016.2580609

41. K. Mathiyalagan, J. H. Park, R. Sakthivel, Synchronization for delayed memristive BAM neural networks using impulsive control with random nonlinearities, *Appl. Math. Comput.*, **259** (2015), 967–979. https://doi.org/10.1016/j.amc.2015.03.022

42. R. Sakthivel, R. Anbuvithya, K. Mathiyalagan, Y. K. Ma, P. Prakash, Reliable anti-synchronization conditions for BAM memristive neural networks with different memductance functions, *Appl. Math. Comput.*, **275** (2016), 213–228. https://doi.org/10.1016/j.amc.2015.11.060

43. Z. Cai, L. H. Huang, Generalized Lyapunov approach for functional differential inclusions, *Automatica*, **113** (2020), 108740. https://doi.org/10.1016/j.automatica.2019.108740

44. Z. Cai, J. Huang, L. H. Huang, Generalized Lyapunov-Razumikhin method for retarded differential inclusions: Applications to discontinuous neural networks, *Discrete Contin. Dyn. Syst. - Ser. B*, **22** (2017), 3591–3614. https://doi.org/10.3934/dcdsb.2017181

45. Z. Cai, L. H. Huang, Lyapunov-Krasovskii stability analysis of delayed Filippov system: Applications to neural networks with switching control, *Int. J. Robust Nonlinear Control*, **30** (2020), 699–718. https://doi.org/10.1002/rnc.4787

46. Z. Cai, L. H. Huang, Z. Wang, Finite-/Fixed-time stability of nonautonomous functional differential inclusion: Lyapunov approach involving indefinite derivative, *IEEE Trans. Neural Networks Learn. Syst.*, **33** (2021), 6763–6774. https://doi.org/10.1109/TNNLS.2021.3083396

47. Z. Y. Guo, L. H. Huang, Generalized Lyapunov method for discontinuous systems, *Nonlinear Anal. Theory Methods Appl.*, **71** (2009), 3083–3092. https://doi.org/10.1016/j.na.2009.01.220

48. J. Cortés, Discontinuous dynamical systems, *IEEE Control Syst. Mag.*, **28** (2008), 36–73. https://doi.org/10.1109/MCS.2008.919306

49. Q. X. Zhu, J. D. Cao, Stability analysis of Markovian jump stochastic BAM neural networks with impulse control and mixed time delays, *IEEE Trans. Neural Networks Learn. Syst.*, **23** (2012), 467–479. https://doi.org/10.1109/TNNLS.2011.2182659

50. M. Forti, M. Grazzini, P. Nistri, L. Pancioni, Generalized Lyapunov approach for convergence of neural networks with discontinuous or non-Lipschitz activations, *Physica D*, **214** (2006), 88–99. https://doi.org/10.1016/j.physd.2005.12.006

51. G. H. Hardy, J. E. Littlewood, G. Polya, *Inequalities*, Cambridge University Press, Cambridge, 1952.

52. Z. Cai, L. H. Huang, Z. Wang, Prespecified-time control of switched neural networks: novel Lyapunov approach of prespecified-time stability, *Comput. Appl. Math.*, **43** (2024), 224. https://doi.org/10.1007/s40314-024-02748-w

53. J. P. Aubin, A. Cellina, *Differential Inclusions: Set-Valued Maps and Viability Theory*, Springer-Verlag, 1984.

AIMS Press